Task Assignment for Multiplayer Reach–Avoid Games in Convex Domains via Analytical Barriers

Rui Yan, *Student Member, IEEE*, Zongying Shi, *Member, IEEE*, and Yisheng Zhong

***Abstract*—This article considers a multiplayer reach–avoid game between two adversarial teams in a general convex domain which consists of a target region and a play region. The evasion team, initially lying in the play region, aims to send as many team members into the target region as possible, while the pursuit team with its team members initially distributed in both play region and target region, strives to prevent that by capturing the evaders. We aim at investigating a task assignment about the pursuer–evader matching, which can maximize the number of the evaders who can be captured before reaching the target region safely when both teams play optimally. To address this, two winning regions for a group of pursuers to intercept an evader are determined by constructing an analytical barrier which divides these two parts. Then, a task assignment to guarantee the most evaders intercepted is provided by solving a simplified 0-1 integer programming instead of a nondeterministic polynomial problem, easing the computation burden dramatically. It is worth noting that except the task assignment, the whole analysis is analytical. Finally, simulation results are also presented.**

***Index Terms*—Barriers, differential games, multiagent systems, optimal control, pursuit–evasion games, reach–avoid (RA) games.**

I. Introduction

THIS article studies a multiplayer reach–avoid (RA) game between two adversarial teams of cooperative players playing in a convex-bounded planar domain, which is partitioned into a target region and a play region by a straight line. Starting from the play region, the evasion team aims to send as many its team members, called evaders, into the target region as possible. Conversely, the pursuit team initially lying in the target region and play region, strives to prevent the evasion team from doing so by attempting to capture the evaders. Actually, from another side, this game can also be viewed as an evasion team trying to escape from a bounded region through an exit which is represented by a straight line, while avoiding adversaries and moving obstacles formulated as a pursuit team. Such a differential game is a powerful theoretical tool for analyzing realistic situations in robotics, aircraft control, security, reachability analysis, and other domains [1]–[5]. For example, in collision avoidance and path planning, how a group of vehicles can get into some target set or escape from a bounded region through an exit, while avoiding dangerous situations, such as collisions with static or moving obstacles is discussed [6]–[8]. In region pursuit games, multiple pursuers are used to intercept multiple adversarial intruders [9]–[11]. In safety verification, an agent often needs to judge whether it can guarantee its arrival into a safe region through plenty of dynamic dangers, such as disturbances and adversaries [12]. In the references [13] and [14], cooperative behaviors within pursuit–evasion games are analyzed in order to help or rescue teammates in the presence of adversarial players.

However, finding cooperative strategies and task assignment among multiple players, especially when two teams both consist of multiple members, can be challenging [15], as computing solutions over the joint state space of multiple players can greatly increase computational complexity, beyond the scope of traditional dynamic programming [1]. In [16], a formal analysis and taxonomy of task allocation in multirobot systems is presented. More recently, a distributed version of the Hungarian method [17] and consensus-based decentralized auction and bundle algorithms [18] are proposed to solve the multirobot assignment problem. The authors in [19] study the problem of multirobot active target tracking by processing relative observations. Due to the conflicting and asymmetric goals between two teams, complex cooperation and nonintuitive strategies within each team may exist. Although some techniques have been used to analyze RA games and demonstrated to work well in some conditions, they are mostly numerical algorithms and suffer from some weaknesses, such as highly computational complexity, conservation, strong assumption and application limitations [20]–[23].

Although the problem considered in this article is different from the classical pursuit–evasion games that have been thoroughly studied, we borrow several existing notions and modify their definitions slightly to address our current scenario. For RA games, as Isaacs' book [24] shows, the core point is to construct the barrier, which is the boundary of the RA set, splitting the entire state space into two disjoint parts: pursuit winning region (PWR) and evasion winning region (EWR). The PWR is the region of initial conditions, from which the pursuit team can ensure the capture before the evader enters the target region. The EWR, complementary to the PWR, is the region of initial conditions, from which the evader can succeed to reach the target region regardless of the pursuit team's strategies.

Manuscript received January 5, 2019; revised June 13, 2019; accepted August 7, 2019. Date of publication September 4, 2019; date of current version February 4, 2020. This work was supported in part by the National Natural Science Foundation of China under Grant 61374034, and in part by China Scholarship Council. This article was recommended for publication by Associate Editor J. Shamma and Editor P. Robuffo Giordano upon evaluation of the reviewers' comments. *(Corresponding author: Zongying Shi.)*

The authors are with the Department of Automation, Tsinghua University, Beijing 100084, China (e-mail: yr15@mails.tsinghua.edu.cn; szy@mail.tsinghua.edu.cn; zys-dau@mail.tsinghua.edu.cn).

Color versions of one or more of the figures in this article are available online at http://ieeexplore.ieee.org.

Digital Object Identifier 10.1109/TRO.2019.2935345

The surface that separates the PWR from the EWR is called barrier.

In principle, the Hamilton–Jacob–Isaacs (HJI) approach is an ideal tool for solving general RA games when the game is low-dimensional, such as autonomous river navigation for underactuated vehicles [25] and safety specifications in hybrid systems [26]. By defining a value function by merging the payoff function and discriminator function with minmax operation, this approach involves solving a HJI partial differential equation (PDE) in the joint state space of the players and locating the barrier by finding the zero sublevel set of this value function. The players' optimal strategies can be extracted from the gradient of the value function. Generally, there are two approaches to solve the HJI PDEs: The method of characteristics [14] and numerical approximation of the value function on a grid of the continuous state space [27]–[29].

However, in practical applications, both the two approaches face computational challenges. Nonunique terminal conditions in RA game setups, capture or entry into the target set, make it difficult to generate strategies by characteristic solutions which require backward integration from terminal manifold, as different backward trajectories may produce complicated singular surfaces for which there exist no systematic analysis methods [30]. On the other hand, a number of numerical tools for solving HJI PDEs on grids have been provided to solve practical problems [28]. Unfortunately, the curse of dimensionality makes these approaches computationally intractable in our multiplayer RA games, as the grid required for approximating the value function scales exponentially with the number of players.

For certain games and game setups, geometric method shows an incredible power in providing strategies for the players [31]–[33]. For example, Voronoi diagrams, dividing a plane into regions of points that are closest to a predetermined set of seed points, are widely used for generating strategies in pursuit–evasion games, usually when each player possesses the same speed. Especially in group pursuit of a single evader or multiple evaders, Voronoi-based approaches can provide very constructive cooperative strategies, such as minimizing the area of the generalized Voronoi partition of the evader [34], [35] or pursuing the evader in a relay way [36]. As for unequal speed scenarios, the Apollonius circle, first introduced by Isaacs, is a useful tool for analyzing the capture of a high-speed evader by using multiple pursuers [37], [38]. More realistically, when pursuit–evasion games are played in the presence of obstacles that inhibit the motions of the players, Euclidean shortest path method is employed to construct the dominance region in [39], and visibility-based target tracking games are addressed in [40] and [41]. The work by Katsev *et al.* [42] introduces a simple wall-following robot to map and solve pursuit–evasion strategies in an unknown polygonal environment. The authors [43] revisit the lion and man problem by introducing line-of-sight visibility. In [44], the number of pursuers which can guarantee to capture an equal speed evader in polygonal environment with obstacles, is investigated. For RA games, a number of straight lines called paths of defense, separating the target set from evaders, are created to compute an approximate dimensional slice of the RA set, which eases the computational burden sharply [9].

The construction of barrier, the most central and important part in RA games, has attracted a lot of attention in pursuit–evasion games and until now, achieved remarkable results [45]–[48]. For example, in [49] and [50], the authors compute the barrier for a pursuit–evasion game between an omnidirectional evader and a differential drive robot. For the problem of tracking an evader in an environment containing a corner, the method of explicit policy is used to investigate the escape set and the track set [51]. In [52], the boundary of RA set is studied for general RA differential games. By adopting the method of characteristics or numerical approximation on grid, the barrier for two players or at most three players is constructed analytically or numerically. However, computing the barrier directly for more than three players in pursuit–evasion games is missing, resulting from the intrinsic high dimensionality of the joint state space.

Compared with the traditional pursuit–evasion games, RA games are more complicated and have more practical significance, as the evaders aim to not only to avoid the capture, but also strive to reach a target set. To our best knowledge, the current article for RA games mainly focuses on the construction of barrier in two-player scenarios [9], [28], [29]. The methods in [9], [28], and [29] are numerical and cannot directly obtain the barrier for multiple players due to the complex cooperation among players and the high computation burden. Additionally, in these works, only one-pursuer-one-evader matching pairs can be obtained, as they only construct the boundary of RA set for one pursuer versus one evader cases. However, in our article, the matching also contains two-pursuer-one-evader matching pairs, in which the evader can only be captured by two pursuers with cooperation while any one of two pursuers cannot capture the evader by itself. The work [38] is most similar to this article, but it only considers two pursuers and one evader cases without involving the complicated cooperation among the pursuit team occurring in this article, and it only focuses on a square game domain which is quite limited. Moreover, our current article also allows the pursuers to start the game in the target region, which is not considered in [38].

In this article, an analytical study on the number of the evaders which the pursuit team would be able to prevent from reaching the target region, is presented by generating a task assignment, namely, pursuer–evader matching pairs. Actually, the above analysis refers to a game of kind [24]. To this end, all pursuers are first classified into all possible coalitions. Then, an evasion region method is proposed to construct the barrier analytically for each pursuit coalition versus one evader in convex domains, which is the first time in the existing literature to construct the barrier directly for multiplayer games with more than three players involved. More importantly, the constructed barrier is analytical and overcomes the curse of dimensionality. Finally, with rich prior information in hand about which evaders can be intercepted by a specified pursuit coalition, a maximum pursuer–evader matching is given such that the most evaders are intercepted.

The contributions of this article are as follows. First, the analytical barrier is constructed for one and two pursuers versus one evader in convex domains. Second, the analytical barrier

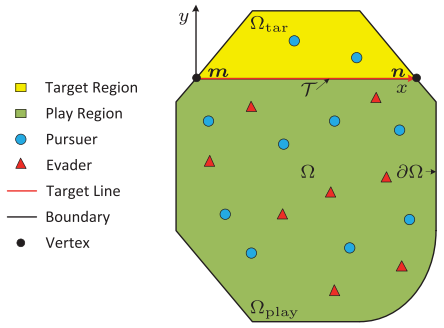

Fig. 1. Multiplayer reach–avoid games in convex domains, where the pursuit team with multiple pursuers (blue circles) wants to capture the most evaders (red triangles) before these evaders enter the target region. Our goal is to find a task assignment for the pursuit team to guarantee the most evaders captured, involving pursuer–evader matching pairs.

for multiple pursuers versus one evader is given, involving two kinds of initial deployments shown in Assumptions 2 and 3, which can determine the capturable and uncapturable regions for these pursuers. Third, since all possible cooperation among the pursuit team is considered, the upper bound on the number of the evaders which the pursuit team can guarantee to intercept, is given by solving a 0-1 integer programming instead of a nondeterministic polynomial problem, greatly easing the computation burden. Fourth, except the task assignment, the whole analysis is analytical, allowing for real-time updates. These contributions provide a complete solution from the perspective of the task assignment to multiplayer RA games in any convex domains consisting of a target region and a play region separated by a straight line.

The rest of this article is organized as follows. In Section II, the problem statement is given. In Section III, some important preliminaries are presented. In Section IV, the barrier and winning regions for one pursuit coalition versus one evader, are found. In Section V, the task assignment for the pursuit team to capture the most evaders, is designed. In Section VI, simulation results are presented. Finally, Section VII concludes this article.

II. Problem Statement

A. Multiplayer Reach–Avoid Games

Consider $N_p + N_e$ players partitioned into two teams, a pursuit team of N_p pursuers, $\{P_i\}_{i=1}^{N_p} = \{P_1, \ldots, P_{N_p}\}$, and an evasion team of N_e evaders, $\{E_j\}_{j=1}^{N_e} = \{E_1, \ldots, E_{N_e}\}$, whose states are constrained in a bounded, convex domain $\Omega \subset \mathbb{R}^2$ with boundary $\partial\Omega$. Each player is assumed to be a mass point. As Fig. 1 shows, a straight line $\mathcal{T} \subset \Omega$, called target line, divides Ω into two disjoint parts Ω_{tar} and Ω_{play}. The compact set Ω_{tar}, called target region, represents the region which the evasion team strives to enter while the pursuit team tries to protect. The play region $\Omega_{\text{play}} = \Omega \setminus \Omega_{\text{tar}}$ corresponds to the region in which two teams play the game. Also note that $\mathcal{T} \subset \Omega_{\text{tar}}$. Let $\mathbf{x}_{P_i}(t) = (x_{P_i}(t), y_{P_i}(t)) \in \mathbb{R}^2$ and $\mathbf{x}_{E_j}(t) = (x_{E_j}(t), y_{E_j}(t)) \in \mathbb{R}^2$ be the positions of P_i and E_j at time t, respectively. The dynamics of the players are described by the following decoupled system for $t \geq 0$:

$$\begin{aligned} \dot{\mathbf{x}}_{P_i}(t) &= v_{P_i}\mathbf{u}_{P_i}(t), \quad \mathbf{x}_{P_i}(0) = \mathbf{x}^0_{P_i}, \quad i = 1, \ldots, N_p \\ \dot{\mathbf{x}}_{E_j}(t) &= v_{E_j}\mathbf{u}_{E_j}(t), \quad \mathbf{x}_{E_j}(0) = \mathbf{x}^0_{E_j}, \quad j = 1, \ldots, N_e \end{aligned} \tag{1}$$

where $\mathbf{x}^0_{P_i} = (x^0_{P_i}, y^0_{P_i}) \in \mathbb{R}^2$ and $\mathbf{x}^0_{E_j} = (x^0_{E_j}, y^0_{E_j}) \in \mathbb{R}^2$ are the initial positions of P_i and E_j, respectively. The maximum speeds of P_i and E_j are denoted by v_{P_i} and v_{E_j} respectively. The control inputs at time t for P_i and E_j are $\mathbf{u}_{P_i}(t)$ and $\mathbf{u}_{E_j}(t)$ respectively, and they satisfy the constraint $\mathbf{u}_{P_i}(t), \mathbf{u}_{E_j}(t) \in \mathcal{U} = \{\mathbf{u} \in \mathbb{R}^2 | \|\mathbf{u}\|_2 = 1\}$, where $\|\cdot\|_2$ stands for the Euclidean norm in $\mathbb{R}^2$. Unless needed for clarity, to simplify notations, t will be omitted hereinafter.

The goal of the evasion team is to send as many evaders as possible into Ω_{tar} without being captured, while the pursuit team strives to prevent the evasion team from that by capturing the evaders. Naturally, once an evader enters Ω_{tar}, the pursuer cannot capture it hereinafter. Assume that E_j is captured by P_i in Ω_{play} if E_j's position coincides with P_i's position, that is, the point-capture is considered. Our article aims to investigate an optimal interception matching scheme for the pursuit team such that the most evaders can be intercepted, and also provide strategy instructions for the evasion team.

In view of the pursuit team's goal, all possible cooperation among the pursuers must be considered, which is not involved in the existing literature on multiplayer RA games. The maximum matching employed by [9] can only provide a suboptimal strategy for the pursuit team, as cooperation is only introduced at the matching step. Since the pursuit team has N_p pursuers, one can select one-pursuer coalitions, two-pursuer coalitions...until N_p-pursuer coalitions, as Fig. 2 shows. Therefore, there are $2^{N_p} - 1$ alternatives for pursuit coalitions among N_p pursuers. These coalitions are labeled from 1 to $2^{N_p} - 1$ successively, so that they can be coded in a binary way as follows.

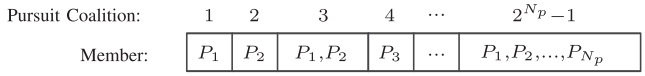

Fig. 2. All possible pursuit coalitions in a pursuit team with N_p pursuers coded in a binary way. For example, the binary code of three is 11, and thus the pursuit coalition 3's members are P_1 and P_2, namely, $m_1 = 1$ and $m_2 = 2$.

Definition 1 (Binary Coalitions for Pursuit Team): $\forall k = 1, \ldots, 2^{N_p} - 1$, P_i belongs to the pursuit coalition k if the ith bit from low order side in binary representation of k is 1. Then, denote the index set of the pursuers in pursuit coalition k by $\mathcal{I}_k = \{m_j | 1 \leq m_j \leq N_p, j = 1, 2, \ldots, n_k\}$ satisfying $m_i < m_j$ for $i < j$, where n_k is the number of the pursuers in pursuit coalition k.

Definition 2 (Pursuit Subcoalition): Consider two pursuit coalitions k_1 and k_2. If every pursuer in k_1 occurs in k_2, then k_1 is called a pursuit subcoalition of k_2.

Obviously, there are plenty of ways to code these pursuit coalitions, but this binary way is very convenient to determine every coalition's members by only recording its number, as Fig. 2 shows. For example, for the pursuit coalition $k = 5$, since the binary representation of five is 101, thus this pursuit coalition's

members are P_1 and P_3, namely, $m_1 = 1$ and $m_2 = 3$. The adoption of pursuit subcoalition will tremendously simplify our problems as discussed as follows.

B. Information Structure and Assumptions

As is the usual convention in the game theory, the equilibrium outcomes crucially depend on the information structure employed by each player. Classically, the state feedback information structure allows each player to choose its current input, $\mathbf{u}_{P_i}$ or $\mathbf{u}_{E_j}$, based on the current value of the information set $\{\mathbf{x}_{P_1}, \ldots, \mathbf{x}_{P_{N_p}}, \mathbf{x}_{E_1}, \ldots, \mathbf{x}_{E_{N_e}}\}$. This article focuses on a nonanticipative information structure, as commonly adopted in the differential game literature (see for example [27], [53]). Under this information structure, the pursuit team is allowed to make decisions about its current input with all the information of state feedback, plus the evasion team's current input. While the evasion team is at a slight disadvantage under this information structure, at a minimum he has access to sufficient information to use state feedback, because the pursuit team must declare his strategy before the evasion team chooses a specific input and thus the evasion team can determine the response of the pursuit team to any input signal. Thus, the multiplayer RA games formulated here are an instantiation of the Stackelberg game [1].

As Fig. 1 shows, let $\boldsymbol{m}$ and $\boldsymbol{n}$ denote the endpoints of $\mathcal{T}$, and assume $\|\boldsymbol{m} - \boldsymbol{n}\|_2 = l$. Fix the origin at $\boldsymbol{m}$, and build a Cartesian coordinate system with x-axis along the straight line through $\boldsymbol{m}$ and $\boldsymbol{n}$, and y-axis perpendicular to x-axis and pointing to Ω_{tar}. For unity, we assume that $\mathbb{R}^n = \mathbb{R}^{1\times n}$, where n is a positive integer.

Next, it is assumed that the following conditions are satisfied by the initial configurations of the players, where Assumptions 2 and 3 will be separately considered.

Assumption 1 (Isolate Initial Deployment): The initial positions of the players satisfy three conditions:

1) $\|\mathbf{x}^0_{P_i} - \mathbf{x}^0_{P_j}\|_2 > 0$ for all $i, j = 1, \ldots, N_p, i \neq j$;
2) $\|\mathbf{x}^0_{E_i} - \mathbf{x}^0_{E_j}\|_2 > 0$ for all $i, j = 1, \ldots, N_e, i \neq j$;
3) $\|\mathbf{x}^0_{P_i} - \mathbf{x}^0_{E_j}\|_2 > 0$ for all $i = 1, \ldots, N_p, j = 1, \ldots, N_e$.

It can be seen that Assumption 1 guarantees that all players start to play the game from different initial positions and every evader is not captured by the pursuers initially.

Assumption 2 (Constrained Initial Deployment): Suppose that $\mathbf{x}^0_{P_i} \in \Omega_{\text{play}} \cup \mathcal{T}$ for all $i = 1, \ldots, N_p$ and $\mathbf{x}^0_{E_j} \in \Omega_{\text{play}}$ for all $j = 1, \ldots, N_e$.

Assumption 3 (Relaxed Initial Deployment): Suppose that $\mathbf{x}^0_{P_i} \in \Omega$ for all $i = 1, \ldots, N_p$ and $\mathbf{x}^0_{E_j} \in \Omega_{\text{play}}$ for all $j = 1, \ldots, N_e$.

In Assumptions 2 and 3, restricting evaders' initial positions into Ω_{play} is a reasonable assumption for our RA games, as the evaders win once they enter Ω_{tar}. As for the initial positions of the pursuers, Assumption 2 is employed out of consideration for developing an extensible basic approach and also for analyzing the capture of evaders before their escaping from a region (i.e., Ω_{play}) by an exit (i.e., $\mathcal{T}$), in which the pursuers usually also lie in this region. Then, the more general initial configurations described in Assumption 3, such as the pursuers are stochastically patrolling in the whole region Ω before the evaders occur, and even sometimes the pursuers rest in their home region (i.e., Ω_{tar}) before the evaders are observed, are investigated by building a bridge to the proposed basic approach. Moreover, an initial deployment is admissible if Assumptions 1 and 2 or 1 and 3 hold.

Generally, in multiplayer RA games, the pursuers are homogeneous and the same for the evaders, such as confrontation between two species, and collision avoidance in the environment with similar dynamic obstacles. Thus, our discussion assumes that the pursuers have the same maximum speed v_P, and the evaders have the same maximum speed v_E.

Assumption 4 (Speed Ratio): Define $\alpha = v_E/v_P$ to be the speed ratio. Suppose that $v_{P_i} = v_P > 0, i = 1, \ldots, N_p$, and $v_{E_j} = v_E > 0, j = 1, \ldots, N_e$. Assume that $0 < \alpha < 1$.

III. Preliminaries

A. Computation of the ER and BER

For $\boldsymbol{x}, \boldsymbol{y} \in \mathbb{R}^2$, define two maps $r(\boldsymbol{x}, \boldsymbol{y}) = \frac{\alpha\|\boldsymbol{x}-\boldsymbol{y}\|_2}{1-\alpha^2}$ and $\eta(\boldsymbol{x}, \boldsymbol{y}) = \frac{\boldsymbol{x}-\alpha^2\boldsymbol{y}}{1-\alpha^2}$ [37], whose geometric meanings will be stated as follows.

Let the set of points in $\mathbb{R}^2$ that one evader can reach before one pursuer, regardless of the pursuer' best effort, be called evasion region (ER), and the surface which bounds ER is called the boundary of ER (BER).

Denote the ER and BER determined by P_i and E_j by $\mathcal{R}_e(\mathbf{x}^0_{E_j}, \mathbf{x}^0_{P_i})$ and $\mathcal{A}(\mathbf{x}^0_{E_j}, \mathbf{x}^0_{P_i})$ respectively, which can be mathematically formulated as follows:

$$\begin{aligned}\mathcal{R}_e &= \left\{\mathbf{z} \in \mathbb{R}^2 | \|\mathbf{z} - \mathbf{x}^0_{E_j}\|_2 < \alpha\|\mathbf{z} - \mathbf{x}^0_{P_i}\|_2\right\}\\ \mathcal{A} &= \left\{\mathbf{z} \in \mathbb{R}^2 | \|\mathbf{z} - \mathbf{x}^0_{E_j}\|_2 = \alpha\|\mathbf{z} - \mathbf{x}^0_{P_i}\|_2\right\}.\end{aligned} \tag{2}$$

Also note that

$$\begin{aligned}&\|\mathbf{z} - \mathbf{x}^0_{E_j}\|_2^2 < \alpha^2\|\mathbf{z} - \mathbf{x}^0_{P_i}\|_2^2\\ &\Rightarrow \|\mathbf{z}\|_2^2 - 2\frac{\left(\mathbf{x}^0_{E_j} - \alpha^2\mathbf{x}^0_{P_i}\right)^{\mathsf{T}}\mathbf{z}}{1-\alpha^2} < \frac{\alpha^2\|\mathbf{x}^0_{P_i}\|_2^2 - \|\mathbf{x}^0_{E_j}\|_2^2}{1-\alpha^2}\\ &\Rightarrow \left\|\mathbf{z} - \frac{\mathbf{x}^0_{E_j} - \alpha^2\mathbf{x}^0_{P_i}}{1-\alpha^2}\right\|_2^2 < \frac{\alpha^2\|\mathbf{x}^0_{E_j} - \mathbf{x}^0_{P_i}\|_2^2}{(1-\alpha^2)^2}\\ &\Rightarrow \left\|\mathbf{z} - \eta\left(\mathbf{x}^0_{E_j}, \mathbf{x}^0_{P_i}\right)\right\|_2^2 < r^2\left(\mathbf{x}^0_{E_j}, \mathbf{x}^0_{P_i}\right)\end{aligned} \tag{3}$$

implying that (2) can be equivalently rewritten as

$$\begin{aligned}\mathcal{R}_e &= \left\{\mathbf{z} \in \mathbb{R}^2 \left| \left\|\mathbf{z} - \eta\left(\mathbf{x}^0_{E_j}, \mathbf{x}^0_{P_i}\right)\right\|_2 < r\left(\mathbf{x}^0_{E_j}, \mathbf{x}^0_{P_i}\right)\right.\right\}\\ \mathcal{A} &= \left\{\mathbf{z} \in \mathbb{R}^2 \left| \left\|\mathbf{z} - \eta\left(\mathbf{x}^0_{E_j}, \mathbf{x}^0_{P_i}\right)\right\|_2 = r\left(\mathbf{x}^0_{E_j}, \mathbf{x}^0_{P_i}\right)\right.\right\}.\end{aligned} \tag{4}$$

Thus, it can be seen that $\mathcal{A}$ is a circle of radius $r(\mathbf{x}^0_{E_j}, \mathbf{x}^0_{P_i})$ centered at $\eta(\mathbf{x}^0_{E_j}, \mathbf{x}^0_{P_i})$, and $\mathcal{R}_e$ is the interior of $\mathcal{A}$, shown in Fig. 3(a). This circle $\mathcal{A}$, also called Apollonius circle [24], divides $\mathbb{R}^2$ into two parts: The interior of the circle is E_j's dominance region, i.e., the ER $\mathcal{R}_e$: E_j can reach any point inside the circle before P_i; the exterior of the circle is P_i's dominance

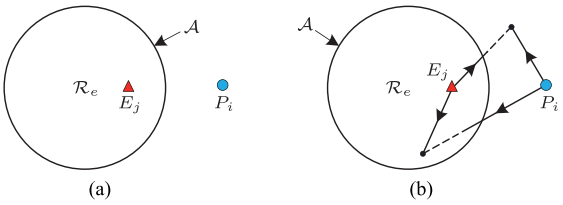

Fig. 3. ER and BER. (a) The ER and BER determined by P_i and E_j are $\mathcal{R}_e$ and $\mathcal{A}$ respectively, where $\mathcal{A}$ is a circle and $\mathcal{R}_e$ is the interior of this circle. (b) The circle $\mathcal{A}$, also called Apollonius circle, divides $\mathbb{R}^2$ into two parts: the interior of the circle is E_j's dominance region, i.e., the ER $\mathcal{R}_e$: E_j can reach any point inside the circle before P_i; the exterior of the circle is P_i's dominance region: P_i can reach any point outside the circle before E_j.

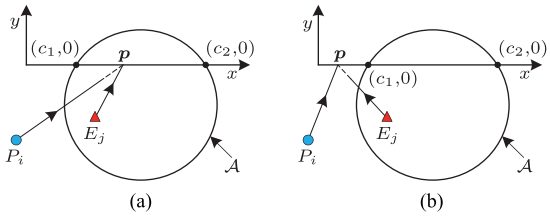

Fig. 4. Monotony of the function $G_1(x_p)$, where $\boldsymbol{p} = (x_p, 0)$ and $G_1(c_1) = G_1(c_2) = 0$. (*a*) If $x_p \in (c_1, c_2)$, $G_1(x_p) > 0$, that is, E_j can reach $\boldsymbol{p}$ before P_i. (*b*) If $x_p \in (-\infty, c_1) \cup (c_2, +\infty)$, $G_1(x_p) < 0$, that is, P_i can reach $\boldsymbol{p}$ before E_j. It is proved that there exists a unique maximum point of $G_1(x_p)$ for $x_p \in [c_1, c_2]$.

region: P_i can reach any point outside the circle before E_j, as Fig. 3(b) illustrates.

Unless needed for clarity, to simplify notations, drop the initial positions occurring in the expressions of $\mathcal{R}_e$ and $\mathcal{A}$.

B. Key Function

Next, present an important lemma about a key function.

Lemma 1 (Monotony of Function): Given P_i and E_j's initial positions $\mathbf{x}^0_{P_i}$ and $\mathbf{x}^0_{E_j}$ satisfying $y^0_{E_j} < 0$ and $x^0_{P_i} \le x^0_{E_j}$, if $\mathcal{A} \cap \{\mathbf{z} \in \mathbb{R}^2 | y = 0\} = \{(c_1, 0), (c_2, 0)\}$ with $c_1 < c_2$, the function

$$G_1(x_p) = \left\|\boldsymbol{p} - \mathbf{x}^0_{P_i}\right\|_2 - \frac{\left\|\boldsymbol{p} - \mathbf{x}^0_{E_j}\right\|_2}{\alpha}, \quad \boldsymbol{p} = (x_p, 0) \tag{5}$$

is strictly monotonically increasing for $x_p \in [c_1, x^*_p]$, and strictly monotonically decreasing for $x_p \in [x^*_p, c_2]$, where x^*_p is the unique solution of the quartic equation

$$\frac{x^*_p - x^0_{P_i}}{\left\|\boldsymbol{p}^* - \mathbf{x}^0_{P_i}\right\|_2} = \frac{x^*_p - x^0_{E_j}}{\alpha\left\|\boldsymbol{p}^* - \mathbf{x}^0_{E_j}\right\|_2}, \quad \boldsymbol{p}^* = (x^*_p, 0) \tag{6}$$

in the interval $[c_1, c_2]$.

Proof: See Fig. 4(a). Take $\boldsymbol{p} = (x_p, 0)$. It can be seen that if $x_p \in [c_1, c_2]$, $G_1(x_p)$ in (5) is actually the distance (depicted in dashed line) between P_i and E_j exactly when E_j arrives at $\boldsymbol{p}$, if P_i and E_j both move directly towards $\boldsymbol{p}$.

Note that $\mathcal{A}$ is a circle. Thus, based on (2), $\mathcal{A} \cap \{\mathbf{z} \in \mathbb{R}^2 | y = 0\} = \{(c_1, 0), (c_2, 0)\}$ with $c_1 < c_2$ implies that $G_1(c_1) = G_1(c_2) = 0$, $G_1(x_p) > 0$ for $x_p \in (c_1, c_2)$, and $G_1(x_p) < 0$ for $x_p \in (-\infty, c_1) \cup (c_2, +\infty)$. Thus, the maximum point x^*_p of $G_1(x_p)$ lies in $[c_1, c_2]$ and satisfies $G_1'(x^*_p) = 0$. If we can verify $G_1'(x^*_p) = 0$ admits a unique solution x^*_p in the interval $[c_1, c_2]$, then the lemma is straightforward. First, the existence of x^*_p in the interval $[c_1, c_2]$ is obvious by noting that $G_1(x_p)$ is continuous in this interval. Next, prove the uniqueness.

Take $\boldsymbol{p}^* = (x^*_p, 0)$. By taking the derivative for (5) with respect to x_p, $G_1'(x^*_p) = 0$ means that (6) holds. There are two cases depending on whether $x^0_{P_i} < x^0_{E_j}$ or $x^0_{P_i} = x^0_{E_j}$, which will be separately discussed as follows.

Consider $x^0_{P_i} < x^0_{E_j}$ first. Since $x^*_p \in [c_1, c_2]$, as Fig. 4(a) shows, we have $G_1(x^*_p) \ge 0$, implying that

$$\left\|\boldsymbol{p}^* - \mathbf{x}^0_{P_i}\right\|_2 \ge \frac{\left\|\boldsymbol{p}^* - \mathbf{x}^0_{E_j}\right\|_2}{\alpha} > \alpha\left\|\boldsymbol{p}^* - \mathbf{x}^0_{E_j}\right\|_2. \tag{7}$$

Then, combining (6) and (7) leads to

$$\left|x^*_p - x^0_{P_i}\right| > \left|x^*_p - x^0_{E_j}\right|. \tag{8}$$

Also note that (6) guarantees that $x^*_p - x^0_{P_i}$ and $x^*_p - x^0_{E_j}$ have the same plus or minus sign. Thus, by also noting that $x^0_{P_i} < x^0_{E_j}$, then (8) means that $x^*_p > x^0_{E_j} > x^0_{P_i}$, as Fig. 4(a) illustrates. Define

$$G_2(x^*_p) = \frac{\left\|\boldsymbol{p}^* - \mathbf{x}^0_{P_i}\right\|_2^2 (x^*_p - x^0_{E_j})^2}{\left\|\boldsymbol{p}^* - \mathbf{x}^0_{E_j}\right\|_2^2 (x^*_p - x^0_{P_i})^2} \tag{9}$$

and thus (6) can be rewritten as $G_2(x^*_p) = \alpha^2$. Since $\alpha^2 < 1$, then $G_2(x^*_p) < 1$, implying that

$$\begin{aligned} &\left\|\boldsymbol{p}^* - \mathbf{x}^0_{E_j}\right\|_2^2 \left(x^*_p - x^0_{P_i}\right)^2 > \left\|\boldsymbol{p}^* - \mathbf{x}^0_{P_i}\right\|_2^2 \left(x^*_p - x^0_{E_j}\right)^2 \\ &\Rightarrow \left(y^0_{E_j}\right)^2 \left(x^*_p - x^0_{P_i}\right)^2 - \left(y^0_{P_i}\right)^2 \left(x^*_p - x^0_{E_j}\right)^2 > 0. \end{aligned} \tag{10}$$

By computing the derivative of $G_2(x^*_p)$ with respect to x^*_p, it can be verified that $G_2(x^*_p)$ is strictly monotonic for x^*_p satisfying (10) and $x^*_p > x^0_{E_j} > x^0_{P_i}$. Thus, $G_2(x^*_p) = \alpha^2$, i.e., $G_1'(x^*_p) = 0$, admits a unique solution x^*_p in the interval $[c_1, c_2]$.

If $x^0_{P_i} = x^0_{E_j}$, (6) implies that $x^*_p = x^0_{E_j} = x^0_{P_i}$ by noting (7). Thus, $G_1'(x^*_p) = 0$ still admits a unique solution x^*_p in this case, and we finish the proof. □

For simplicity of description, in Lemma 1, only $x^0_{P_i} \le x^0_{E_j}$ is considered. As for $x^0_{P_i} > x^0_{E_j}$, the similar conclusion can be obtained.

IV. One Pursuit Coalition Versus One Evader

A. Problem Formulation

Before investigating the number of the evaders which would be captured in Ω_{play} before entering Ω_{tar}, a subgame between a pursuit coalition k and E_j is analyzed as a building block. Denote the joint game domain for the pursuit coalition k by $\Omega^{n_k} = \Omega \times \cdots \times \Omega$. Similarly, denote the joint play region, target region, target line, and control constraint for the pursuit coalition k by $\Omega^{n_k}_{\text{play}}, \Omega^{n_k}_{\text{tar}}, \mathcal{T}^{n_k}$, and $\mathcal{U}^{n_k}$, respectively. Denote the joint control input and initial state of the pursuit coalition k by $\mathcal{P}_k = \{\mathbf{u}_{P_{m_1}}, \ldots, \mathbf{u}_{P_{m_{n_k}}}\} \in \mathcal{U}^{n_k}$ and $\mathcal{X}^0_k = \{\mathbf{x}^0_{P_{m_1}}, \ldots, \mathbf{x}^0_{P_{m_{n_k}}}\} \in \mathbb{R}^{2n_k}$, respectively.

In order to develop a basic approach, we first restrict $\mathcal{X}_k^0 \in \Omega_{\text{play}}^{n_k} \cup \mathcal{T}^{n_k}$ in Sections IV-C and IV-D, that is, all pursuers initially lie in the play region Ω_{play} or target line $\mathcal{T}$ as Assumption 2 states. Then, the case $\mathcal{X}_k^0 \in \Omega^{n_k}$, that is, all pursuers can start the game from any positions in Ω as Assumption 3 states, will be discussed in Section IV-E. For clarity of the description, k refers to the pursuit coalition k.

Given Ω and $\mathcal{T}$, namely, specifying Ω_{tar} and Ω_{play}, the following problems will be addressed in this section.

Problem 1: Consider k and E_j. Given $\mathcal{X}_k^0$, find the region $\mathcal{W}_P^{n_k}(\mathcal{X}_k^0) \subset \Omega_{\text{play}}$ in which if E_j initially lies, there exists a joint pursuit control input $\mathcal{P}_k \in \mathcal{U}^{n_k}$ such that E_j can be captured before entering Ω_{tar} regardless of its evasion control input $\mathbf{u}_{E_j} \in \mathcal{U}$.

Problem 2: Consider k and E_j. Given $\mathcal{X}_k^0$, find the region $\mathcal{W}_E^{n_k}(\mathcal{X}_k^0) \subset \Omega_{\text{play}}$ in which if E_j initially lies, an evasion control input $\mathbf{u}_{E_j} \in \mathcal{U}$ exists such that E_j can enter Ω_{tar} without being captured regardless of the joint pursuit control $\mathcal{P}_k \in \mathcal{U}^{n_k}$.

Thus, $\mathcal{W}_P^{n_k}(\mathcal{X}_k^0)$ and $\mathcal{W}_E^{n_k}(\mathcal{X}_k^0)$ are the respective winning regions for k and E_j, and we call them PWR and EWR respectively. According to Isaacs' book [24], the barrier, denoted by $\mathcal{B}^{n_k}(\mathcal{X}_k^0)$, is the surface separating $\mathcal{W}_P^{n_k}(\mathcal{X}_k^0)$ from $\mathcal{W}_E^{n_k}(\mathcal{X}_k^0)$, on which no team can guarantee its own winning. In this case, $\mathcal{B}^{n_k}(\mathcal{X}_k^0)$ is a curve, and $\mathcal{B}^{n_k}(\mathcal{X}_k^0) \cup \mathcal{W}_P^{n_k}(\mathcal{X}_k^0) \cup \mathcal{W}_E^{n_k}(\mathcal{X}_k^0) = \Omega_{\text{play}}$. Unless needed for clarity, the initial condition occurring in the expressions of the barrier and winning regions will be dropped from now on.

More visually, given $\mathcal{X}_k^0$, the winning region $\mathcal{W}_P^{n_k}$ can be interpreted as the capturable region of k when facing one evader, while the winning region $\mathcal{W}_E^{n_k}$ corresponds to its uncapturable region. Note that if $\mathcal{B}^{n_k}$ can be obtained, $\mathcal{W}_P^{n_k}$ and $\mathcal{W}_E^{n_k}$ split by $\mathcal{B}^{n_k}$ will come out immediately. As proved later, $\mathcal{B}^{n_k}$ is a continuous or discontinuous curve, dividing Ω_{play} into several subregions. The subregion with $\mathcal{T}$ as its boundary is $\mathcal{W}_E^{n_k}$, and the remaining subregion(s) forms $\mathcal{W}_P^{n_k}$, as Fig. 5(b) shows. Thus, the primary focus in this section is to construct the barrier $\mathcal{B}^{n_k}$.

For a clear symbol description, $\mathcal{B}^{n_k}(\mathcal{X}_k^0)$ is the barrier determined by k with the initial position $\mathcal{X}_k^0$ and n_k pursuers. More generally, $\mathcal{B}^{n_k-1}(\mathcal{X}_k^0 \setminus \mathbf{x}_{P_i}^0)$ denotes the barrier determined by a pursuit coalition with the initial position $\mathcal{X}_k^0 \setminus \mathbf{x}_{P_i}^0$ and $n_k - 1$ pursuers, where $\mathcal{X}_k^0 \setminus \mathbf{x}_{P_i}^0$ denotes the remainder in $\mathcal{X}_k^0$ when $\mathbf{x}_{P_i}^0$ is removed. The similar notations are also applied for $\mathcal{W}_P^{n_k}$ and $\mathcal{W}_E^{n_k}$.

Let $\breve{\mathcal{B}}^{n_k}, \breve{\mathcal{W}}_P^{n_k}$, and $\breve{\mathcal{W}}_E^{n_k}$ respectively denote the barrier, PWR, and EWR of k when the boundary of Ω_{play} is ignored, which will be used to construct $\mathcal{B}^{n_k}, \mathcal{W}_P^{n_k}$, and $\mathcal{W}_E^{n_k}$. These three new notations have the similar meanings, citation ways and notation expressions as $\mathcal{B}^{n_k}, \mathcal{W}_P^{n_k}$, and $\mathcal{W}_E^{n_k}$ respectively, and the only difference is that they are used without considering the boundary of Ω_{play}. They are introduced only for a clear proof.

To clarify clearly, all pursuers in k are classified into two categories from the perspective of these pursuers' relative positions, which plays a crucial role in barrier construction.

Definition 3 (Active and Inactive Pursuers): For a pursuer P_i $(i \in \mathcal{I}_k)$ in k, if there exists at least one point in $\mathcal{T}$ that P_i can reach before all other pursuers in k, we call P_i an active pursuer in k. Otherwise, we call P_i an inactive pursuer in k.

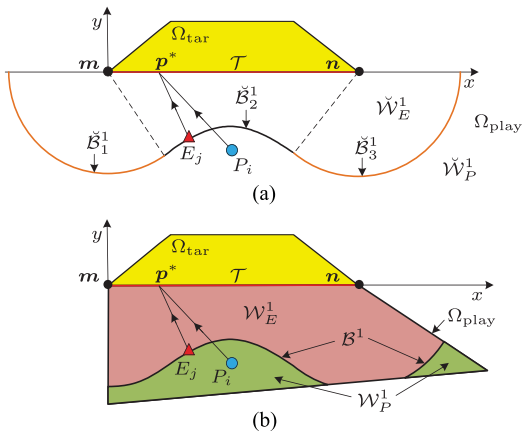

Fig. 5. Barrier and two winning regions determined by P_i when playing with E_j. (a) Without considering the boundary of Ω_{play}, the barrier $\breve{\mathcal{B}}^1$ consists of three curves: $\breve{\mathcal{B}}_1^1$ (orange), $\breve{\mathcal{B}}_2^1$ (black), and $\breve{\mathcal{B}}_3^1$ (orange). The barrier $\breve{\mathcal{B}}^1$ splits Ω_{play} into two winning regions $\breve{\mathcal{W}}_P^1$ and $\breve{\mathcal{W}}_E^1$. If E_j lies in $\breve{\mathcal{W}}_P^1$, P_i can capture E_j before the latter reaches $\mathcal{T}$, while if E_j lies in $\breve{\mathcal{W}}_E^1$, he can guarantee his arrival in $\mathcal{T}$. If E_j lies in $\breve{\mathcal{B}}^1$, under two players' optimal strategies, E_j is captured by P_i exactly when reaching $\mathcal{T}$. (b) By considering the boundary of Ω_{play}, $\mathcal{B}^1$ is given by $\breve{\mathcal{B}}^1 \cap \Omega_{\text{play}}$, as the optimal trajectories for P_i and E_j are both straight lines and Ω_{play} is convex. Naturally, $\breve{\mathcal{W}}_P^1$ becomes the green region $\mathcal{W}_P^1$, and $\breve{\mathcal{W}}_E^1$ becomes the red region $\mathcal{W}_E^1$.

Remark 1: As illustrated in the following, whether a pursuer is active or inactive in a pursuit coalition strictly depends on if it contributes to the barrier construction of this pursuit coalition. In brief, the contribution means being active. It can be noted that a pursuer who is inactive in one pursuit coalition may be active in another pursuit coalition, and vice versa.

We introduce a critical payoff function which is employed to construct the barrier and provides strategies for the players.

Definition 4 (Payoff Function): For k and E_j, if E_j can succeed to reach $\mathcal{T}$, take the distance of E_j to the closest pursuer exactly when E_j arrives at $\mathcal{T}$ as the payoff function. This payoff function J and the associated value function V are respectively given by

$$J = \min_{i \in \mathcal{I}_k} \|\mathbf{x}_{P_i}(t_1) - \mathbf{x}_{E_j}(t_1)\|_2, \quad V = \min_{\mathcal{P}_k \in \mathcal{U}^{n_k}} \max_{\mathbf{u}_{E_j} \in \mathcal{U}} J \quad (11)$$

where t_1 is the first arrival time when E_j reaches $\mathcal{T}$.

The above payoff function, which is also called safe distance on arrival, can be interpreted as E_j desires to reach $\mathcal{T}$ under the safest condition, while k wants to approach E_j as close as possible although the capture cannot be guaranteed.

B. Base Curves

In the construction of the barrier below, the following base curves are utilized, which are very essential to characterize the barrier. We emphasize that the parameters $\boldsymbol{h}_1, \boldsymbol{h}_2$, and $\boldsymbol{h}_3$ defined as follows represent the initial positions of three different pursuers.

Definition 5 (Base Curves): For $\boldsymbol{h}_1 = (x_1,\ y_1), \boldsymbol{h}_2 = (x_2,\ y_2)$ and $\boldsymbol{h}_3 = (x_3, y_3)$ satisfying $y_i \le 0$ $(i = 1, 2, 3)$ and $x_1 < x_2 < x_3$, define the following curves.

1) One Pursuer Case:

$$\begin{aligned}
F_1^1(\boldsymbol{h}_1) &= \big\{\mathbf{z} = (x,y) \in \mathbb{R}^2 | \|\mathbf{z} - \boldsymbol{m}\|_2 \\
&\qquad = \alpha\|\boldsymbol{h}_1 - \boldsymbol{m}\|_2, x \le k_1, \quad y < 0\big\} \\
F_2^1(\boldsymbol{h}_1) &= \big\{\mathbf{z} = (x,y) \in \mathbb{R}^2 | (x - x_1)^2 \\
&\qquad + (1 - 1/\alpha^2)y^2 + (1-\alpha^2)y_1^2 = 0, \\
&\qquad\qquad x \in (k_1, k_2), \quad y < 0\big\} \\
F_3^1(\boldsymbol{h}_1) &= \big\{\mathbf{z} = (x,y) \in \mathbb{R}^2 | \|\mathbf{z} - \boldsymbol{n}\|_2 \\
&\qquad = \alpha\|\boldsymbol{h}_1 - \boldsymbol{n}\|_2, x \ge k_2, \quad y < 0\big\}
\end{aligned} \tag{12}$$

where $k_1 = \alpha^2 x_1$ and $k_2 = (1-\alpha^2)l + \alpha^2 x_1$.

2) Two Pursuers Case:

$$\begin{aligned}
F_1^2(\boldsymbol{h}_1, \boldsymbol{h}_2) &= F_1^1(\boldsymbol{h}_1) \\
F_2^2(\boldsymbol{h}_1, \boldsymbol{h}_2) &= \big\{\mathbf{z} = (x,y) \in \mathbb{R}^2 | (x - x_1)^2 \\
&\qquad + (1 - 1/\alpha^2)y^2 + (1-\alpha^2)y_1^2 = 0, \\
&\qquad\qquad x \in (k_3, k_4), \quad y < 0\big\} \\
F_3^2(\boldsymbol{h}_1, \boldsymbol{h}_2) &= \big\{\mathbf{z} = (x,y) \in \mathbb{R}^2 | \|\mathbf{z} - \boldsymbol{p}_c\|_2 \\
&\qquad = \alpha\|\boldsymbol{h}_1 - \boldsymbol{p}_c\|_2, \quad x \in [k_4, k_5], \quad y < 0\big\} \\
F_4^2(\boldsymbol{h}_1, \boldsymbol{h}_2) &= \big\{\mathbf{z} = (x,y) \in \mathbb{R}^2 | (x - x_2)^2 \\
&\qquad + (1 - 1/\alpha^2)y^2 + (1-\alpha^2)y_2^2 = 0, \\
&\qquad\qquad x \in (k_5, k_6), \quad y < 0\big\} \\
F_5^2(\boldsymbol{h}_1, \boldsymbol{h}_2) &= F_3^1(\boldsymbol{h}_2)
\end{aligned} \tag{13}$$

where $\boldsymbol{p}_c = (x_c, 0)$ is the unique point on the x-axis such that $\|\boldsymbol{p}_c - \boldsymbol{h}_1\|_2 = \|\boldsymbol{p}_c - \boldsymbol{h}_2\|_2$. Here, $k_3 = \alpha^2 x_1$, $k_4 = (1-\alpha^2)x_c + \alpha^2 x_1, k_5 = (1-\alpha^2)x_c + \alpha^2 x_2$ and $k_6 = (1-\alpha^2)l + \alpha^2 x_2$.

3) Three Pursuers Case:

$$\begin{aligned}
F^3(\boldsymbol{h}_1, \boldsymbol{h}_2, \boldsymbol{h}_3) &= \big\{\mathbf{z} = (x,y) \in \mathbb{R}^2 | (x - x_2)^2 \\
&\qquad + (1 - 1/\alpha^2)y^2 + (1-\alpha^2)y_2^2 = 0, \\
&\qquad\qquad x \in (k_7, k_8), \quad y < 0\big\}
\end{aligned} \tag{14}$$

where $k_7 = (1-\alpha^2)x_{c1} + \alpha^2 x_2$ and $k_8 = (1-\alpha^2)x_{c2} + \alpha^2 x_2$. Two points $\boldsymbol{p}_{c1} = (x_{c1}, 0)$ and $\boldsymbol{p}_{c2} = (x_{c2}, 0)$ are respectively given by $\|\boldsymbol{h}_1 - \boldsymbol{p}_{c1}\|_2 = \|\boldsymbol{h}_2 - \boldsymbol{p}_{c1}\|_2$ and $\|\boldsymbol{h}_2 - \boldsymbol{p}_{c2}\|_2 = \|\boldsymbol{h}_3 - \boldsymbol{p}_{c2}\|_2$. Although it is called three pursuers case, F^3 only depends on $\boldsymbol{h}_2$ while the roles of $\boldsymbol{h}_1$ and $\boldsymbol{h}_3$ are to decide two boundaries k_7 and k_8 for x. Thus, each point on F^3 only depends on at most two pursuers by cutting F^3 into two parts.

Remark 2: It can be verified that given $\boldsymbol{h}_1, \boldsymbol{h}_2$, and $\boldsymbol{h}_3$, all base curves are explicit and smooth if they are not empty. Actually, the following discussion will show that the barrier, a focus in our article, is composed by these curves. How to use these base curves will be stated clearly in the next section.

C. Two Pursuers Versus One Evader

We begin the discussion of barrier construction by focusing on an important class of RA subgames with two pursuers and one evader, namely, when k contains two pursuers P_{i1} and P_{i2}. Focusing on this special case enables us to develop a scalable and analytical barrier, while also providing key insights into the barrier construction for general pursuit coalitions.

When Ω_{play} is square, the barrier $\mathcal{B}^2$ can be computed by the method proposed in [38]. However, the shape of Ω_{play} in our current case is convex and not only restricted to square, which is beyond the scope of the previous work while quite common in general RA games. Our current article also allows the pursuers to start the game from Ω_{tar} as Section IV-E shows, which is not involved in [38].

Next, we present a necessary condition that the optimal trajectories should satisfy if the players adopt their optimal strategies from (11).

Lemma 2 (Optimal Trajectories): For P_i and E_j, consider the payoff function (11) when only $\mathbf{x}_{P_i}^0$ $(i \in \mathcal{I}_k)$ is considered in $\mathcal{X}_k^0$. Then, the optimal trajectories for P_i and E_j are both straight lines.

Proof: The Hamiltonian function for this problem is $H = v_P \mathbf{u}_{P_i} \lambda_1^{\mathsf{T}} + v_E \mathbf{u}_{E_j} \lambda_2^{\mathsf{T}}$, where $\lambda_1 \in \mathbb{R}^2$ and $\lambda_2 \in \mathbb{R}^2$ are costate vectors. Therefore, based on the classical Issacs's method, the optimal controls $\mathbf{u}_{P_i}^*$ and $\mathbf{u}_{E_j}^*$ satisfy

$$\mathbf{u}_{P_i}^* = -\frac{\lambda_1}{\|\lambda_1\|_2}, \quad \mathbf{u}_{E_j}^* = \frac{\lambda_2}{\|\lambda_2\|_2}, \quad \dot{\lambda}_1 = 0, \quad \dot{\lambda}_2 = 0. \tag{15}$$

Thus, the optimal controls $\mathbf{u}_{P_i}^*$ and $\mathbf{u}_{E_j}^*$ are time-invariant, and their optimal trajectories are straight lines. □

First, consider the case when k contains only one pursuer, i.e., $\mathcal{X}_k^0 = \mathbf{x}_{P_i}^0$ $(1 \le i \le N_p)$.

Theorem 1 (Barrier for One Pursuer): Consider the system (1) satisfying Assumptions 1, 2, and 4. If a pursuit coalition k only contains one pursuer P_i, then $\mathcal{B}^1(\mathcal{X}_k^0) = \breve{\mathcal{B}}^1 \cap \Omega_{\text{play}}$, where $\breve{\mathcal{B}}^1 = \cup_{s=1}^3 \breve{\mathcal{B}}_s^1$ and $\breve{\mathcal{B}}_s^1 = F_s^1(\mathbf{x}_{P_i}^0)$ for all $s = 1, 2, 3$.

Proof: Since k only contains one pursuer P_i, according to Definition 1, we have $\mathcal{X}_k^0 = \mathbf{x}_{P_i}^0$, $n_k = 1$, and $\mathcal{I}_k = m_1 = i$. Assumption 2 confines $\mathbf{x}_{P_i}^0$ in $\Omega_{\text{play}} \cup \mathcal{T}$. First, we do not consider the boundary of Ω_{play}, namely, focus on the computation of $\breve{\mathcal{B}}^1$ defined in Section IV-A which is proved to consist of three parts $\breve{\mathcal{B}}_1^1, \breve{\mathcal{B}}_2^1$, and $\breve{\mathcal{B}}_3^1$ in the following discussion, as depicted in Fig. 5(a).

Assume that E_j can succeed to reach $\mathcal{T}$, and denote E_j's optimal target point (OTP) in $\mathcal{T}$ by $\boldsymbol{p}^* = (x_p^*, 0)$ such that J in (11) is maximized. It can be seen that in this case, (11) is simplified to

$$J = \|\mathbf{x}_{P_i}(t_1) - \mathbf{x}_{E_j}(t_1)\|_2, \quad V = \min_{\mathbf{u}_{P_i} \in \mathcal{U}} \max_{\mathbf{u}_{E_j} \in \mathcal{U}} J \tag{16}$$

where t_1 is the first arrival time when E_j reaches $\mathcal{T}$.

It follows from Lemma 2 that for the payoff function (16), the optimal trajectories for P_i and E_j are both straight lines. Also note that the nonanticipative information structure stated in Section II-B implies that P_i knows E_j's current input (i.e., direction of motion). Since P_i aims to minimize J in (16), the

optimal strategy for P_i is to move towards the same target point in $\mathcal{T}$ as E_j does, as Fig. 5(a) illustrates. In other words, P_i moves towards the intersection point between $\mathcal{T}$ and the straight line emanating from E_j along E_j's current direction of motion, where the intersection point exists as E_j hopes to reach Ω_{tar}. Hence, if E_j selects $\boldsymbol{p}$ in $\mathcal{T}$ to go, the payoff function J in (16) is equivalent to the function

$$G_1(x_p) = \left\|\boldsymbol{p} - \mathbf{x}_{P_i}^0\right\|_2 - \frac{\left\|\boldsymbol{p} - \mathbf{x}_{E_j}^0\right\|_2}{\alpha}, \quad \boldsymbol{p} = (x_p, 0) \in \mathcal{T} \tag{17}$$

which is P_i's distance to E_j exactly when E_j arrives at $\boldsymbol{p}$, if P_i and E_j both move directly towards $\boldsymbol{p}$. Notice that $0 \le x_p \le l$, where l is the length of $\mathcal{T}$.

Note that E_j strives to maximize J, i.e., $G_1(x_p)$, as (16) shows. Thus, if P_i and E_j both adopt their optimal strategies, x_p^* must be a maximum point of $G_1(x_p)$ for $x_p \in [0, l]$. Note that the monotony of $G_1(x_p)$ has been shown in Lemma 1. If the maximum point x_p^* of $G_1(x_p)$ for $x_p \in [0, l]$ occurs in the interior of $[0, l]$, i.e., $(0, l)$, then x_p^* is an extreme point of $G_1(x_p)$, that is

$$\frac{\mathrm{d}G_1(x_p^*)}{\mathrm{d}x_p} = 0 \Rightarrow \frac{x_p^* - x_{P_i}^0}{\|\boldsymbol{p}^* - \mathbf{x}_{P_i}^0\|_2} = \frac{x_p^* - x_{E_j}^0}{\alpha\|\boldsymbol{p}^* - \mathbf{x}_{E_j}^0\|_2}. \tag{18}$$

Furthermore, assume $\mathbf{x}_{E_j}^0 \in \breve{\mathcal{B}}^1$, as Fig. 5(a) shows. Then, E_j will be captured by P_i exactly when reaching $\mathcal{T}$ under two players' optimal strategies from (16), namely, $V = 0$. Thus, P_i and E_j will reach $\boldsymbol{p}^*$ simultaneously as follows:

$$G_1(x_p^*) = 0 \Rightarrow \left\|\boldsymbol{p}^* - \mathbf{x}_{E_j}^0\right\|_2 = \alpha\left\|\boldsymbol{p}^* - \mathbf{x}_{P_i}^0\right\|_2. \tag{19}$$

This feature (19) reflects that when $\mathbf{x}_{E_j}^0 \in \breve{\mathcal{B}}^1$, under two players' optimal strategies from (16), no player can guarantee its winning, namely, the capture and arrival happen at the same time.

The following analysis will separately consider three cases: $x_p^* \in (0, l)$, $x_p^* = 0$ and $x_p^* = l$, due to their different features.

First, consider $x_p^* \in (0, l)$. It has been shown above that in this case, x_p^* is an extreme point of $G_1(x_p)$. Denote this part of $\breve{\mathcal{B}}^1$ by $\breve{\mathcal{B}}_2^1$ which is in black shown in Fig. 5(a). Next, we compute the expression of $\breve{\mathcal{B}}_2^1$.

Substituting (19) into (18) yields

$$\alpha^2\left(x_p^* - x_{P_i}^0\right) = x_p^* - x_{E_j}^0 \Rightarrow x_p^* = \frac{x_{E_j}^0 - \alpha^2 x_{P_i}^0}{1 - \alpha^2}. \tag{20}$$

Then, substituting x_p^* given by (20) into (19) leads to

$$\begin{aligned}
&\left\|\left(\frac{x_{E_j}^0 - \alpha^2 x_{P_i}^0}{1 - \alpha^2}, 0\right) - \mathbf{x}_{E_j}^0\right\|_2^2 \\
&= \alpha^2\left\|\left(\frac{x_{E_j}^0 - \alpha^2 x_{P_i}^0}{1 - \alpha^2}, 0\right) - \mathbf{x}_{P_i}^0\right\|_2^2 \\
&\Rightarrow \left(x_{E_j}^0 - x_{P_i}^0\right)^2 + (1 - 1/\alpha^2)\left(y_{E_j}^0\right)^2 + (1 - \alpha^2)\left(y_{P_i}^0\right)^2 = 0
\end{aligned} \tag{21}$$

which characterizes the relationship between the initial positions of P_i and E_j when $\mathbf{x}_{E_j}^0 \in \breve{\mathcal{B}}_2^1$. Since $x_p^* \in (0, l)$, (20) implies

$$x_{E_j}^0 \in \left(\alpha^2 x_{P_i}^0, (1 - \alpha^2)l + \alpha^2 x_{P_i}^0\right). \tag{22}$$

Also note that Assumption 2 confines $\mathbf{x}_{E_j}^0$ in Ω_{play}, that is, $y_{E_j}^0 < 0$. Hence, given $\mathbf{x}_{P_i}^0$, by taking all positions $\mathbf{x}_{E_j}^0$ satisfying (21) and (22) with $y_{E_j}^0 < 0$, all initial positions of E_j lying in $\breve{\mathcal{B}}_2^1$ are found. Equivalently, these initial positions of E_j form the $\breve{\mathcal{B}}_2^1$. Thus, by replacing $\mathbf{x}_{E_j}^0$ with a general variable $\mathbf{z} \in \mathbb{R}^2$, it follows from (21), (22) and $y_{E_j}^0 < 0$ that $\breve{\mathcal{B}}_2^1$ is as follows:

$$\begin{aligned}
\breve{\mathcal{B}}_2^1 = \big\{\mathbf{z} = (x, y) \in \mathbb{R}^2 | &(x - x_{P_i}^0)^2 + (1 - 1/\alpha^2)y^2 \\
&+ (1 - \alpha^2)(y_{P_i}^0)^2 = 0, x \in (k_1, k_2), \quad y < 0\big\}
\end{aligned} \tag{23}$$

where $k_1 = \alpha^2 x_{P_i}^0$ and $k_2 = (1 - \alpha^2)l + \alpha^2 x_{P_i}^0$. For clarity, it can be seen that $\breve{\mathcal{B}}_2^1$ can be expressed by a base curve in (12), that is, $\breve{\mathcal{B}}_2^1 = F_2^1(\mathbf{x}_{P_i}^0)$.

Then, we focus on the case $x_p^* = 0$, namely, $\boldsymbol{p}^* = \boldsymbol{m}$. Denote this part of $\breve{\mathcal{B}}^1$ by $\breve{\mathcal{B}}_1^1$ which is the left orange curve in Fig. 5(a). Next, we compute the expression of $\breve{\mathcal{B}}_1^1$.

In this scenario, (19) still holds and becomes

$$\left\|\mathbf{x}_{E_j}^0 - \boldsymbol{m}\right\|_2 = \alpha\left\|\mathbf{x}_{P_i}^0 - \boldsymbol{m}\right\|_2. \tag{24}$$

Note that $x_{E_j}^0 \le \alpha^2 x_{P_i}^0$ is straightforward based on the interval (22) of $x_{E_j}^0$ for $\mathbf{x}_{E_j}^0 \in \breve{\mathcal{B}}_2^1$ and the monotony of $G_1(x_p)$ given by Lemma 1, as Fig. 5(a) shows. Thus, by replacing $\mathbf{x}_{E_j}^0$ with a general variable $\mathbf{z} \in \mathbb{R}^2$, it follows from (24) and $x_{E_j}^0 \le \alpha^2 x_{P_i}^0$ that $\breve{\mathcal{B}}_1^1$ is as follows:

$$\begin{aligned}
\breve{\mathcal{B}}_1^1 = \big\{\mathbf{z} = (x, y) \in \mathbb{R}^2 | &\|\mathbf{z} - \boldsymbol{m}\|_2 \\
&= \alpha\|\mathbf{x}_{P_i}^0 - \boldsymbol{m}\|_2, x \le k_1, \quad y < 0\big\}
\end{aligned} \tag{25}$$

which can also be represented by a base curve in (12), that is, $\breve{\mathcal{B}}_1^1 = F_1^1(\mathbf{x}_{P_i}^0)$.

If $x_p^* = l$, namely, $\boldsymbol{p}^* = \boldsymbol{n}$, denote this part of $\breve{\mathcal{B}}^1$ by $\breve{\mathcal{B}}_3^1$ which is the right orange curve in Fig. 5(a). Similar to the case $x_p^* = 0$, $\breve{\mathcal{B}}_3^1$ is as follows:

$$\begin{aligned}
\breve{\mathcal{B}}_3^1 = \big\{\mathbf{z} = (x, y) \in \mathbb{R}^2 | &\|\mathbf{z} - \boldsymbol{n}\|_2 \\
&= \alpha\|\mathbf{x}_{P_i}^0 - \boldsymbol{n}\|_2, x \ge k_2, \quad y < 0\big\}.
\end{aligned} \tag{26}$$

Thus, $\breve{\mathcal{B}}_3^1 = F_3^1(\mathbf{x}_{P_i}^0)$ can be obtained.

Therefore, we have constructed the barrier $\breve{\mathcal{B}}^1 = \cup_{s=1}^3 \breve{\mathcal{B}}_s^1$, without considering the boundary of Ω_{play}, shown in Fig. 5(a). Then, consider the effect of the boundary of Ω_{play}. Since the optimal trajectories for two players are both straight lines and Ω_{play} is convex, it can be concluded that $\mathcal{B}^1 = \breve{\mathcal{B}}^1 \cap \Omega_{\text{play}}$, as Fig. 5(b) shows. The shape of Ω_{play} in Fig. 5(b), which is general, is introduced just for showing that this theorem is applied for any convex Ω_{play}.

As depicted in Fig. 5(b), since $\mathcal{W}_P^1$ and $\mathcal{W}_E^1$ are two subregions of Ω_{play} and separated by $\mathcal{B}^1$, and $\mathcal{W}_E^1$ is closer to $\mathcal{T}$ than $\mathcal{W}_P^1$,

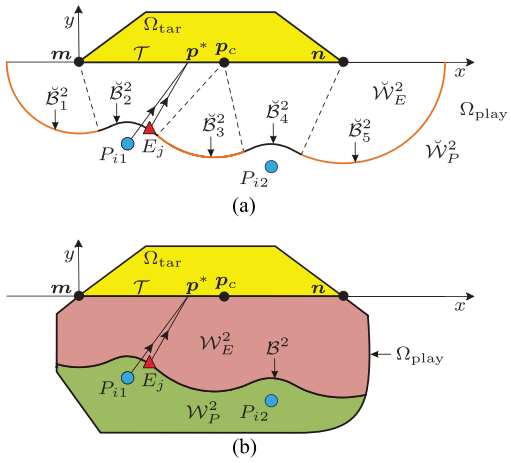

Fig. 6. Barrier and two winning regions determined by two active pursuers P_{i1} and P_{i2} when playing with E_j, in which two pursuers both contribute to the construction of $\breve{\mathcal{B}}^2$. (a) Without considering the boundary of Ω_{play}, the barrier $\breve{\mathcal{B}}^2$ consists of five parts and is given by $\cup_{s=1}^5 \breve{\mathcal{B}}_s^2$. Two winning regions $\breve{\mathcal{W}}_P^2$ and $\breve{\mathcal{W}}_E^2$ for each team's guaranteed winning are split by $\breve{\mathcal{B}}^2$. (b) By considering the boundary of Ω_{play}, $\mathcal{B}^2$ is given by $\breve{\mathcal{B}}^2 \cap \Omega_{\text{play}}$, as the optimal trajectories for the players who work in the payoff function, are straight lines and Ω_{play} is convex. Naturally, $\breve{\mathcal{W}}_P^2$ becomes the green region $\mathcal{W}_P^2$, and $\breve{\mathcal{W}}_E^2$ becomes the red region $\mathcal{W}_E^2$.

then the green region is the PWR $\mathcal{W}_P^1$ and the red region is the EWR $\mathcal{W}_E^1$. Thus, we finish the proof. □

Next, we consider the case when k contains two pursuers, i.e., $\mathcal{X}_k^0 = \{\mathbf{x}_{P_{i1}}^0, \mathbf{x}_{P_{i2}}^0\}$ $(1 \le i1, i2 \le N_p, i1 \ne i2)$. The main result of this section is presented as follows, which gives the analytical barrier for two pursuers case.

Theorem 2 (Barrier for Two Pursuers): Consider the system (1) and suppose that Assumptions 1, 2, and 4 hold. If a pursuit coalition k contains two pursuers P_{i1} and P_{i2}, its barrier can be analytically calculated as follows.

a) (Only one active pursuer). If only P_i is an active pursuer, $\mathcal{B}^2(\mathcal{X}_k^0) = \mathcal{B}^1(\mathbf{x}_{P_i}^0)$ where $i = i1$ or $i2$.
b) (Two active pursuers). If P_{i1} and P_{i2} are both active pursuers, assume $x_{P_{i1}}^0 < x_{P_{i2}}^0$. Then, $\mathcal{B}^2(\mathcal{X}_k^0) = \breve{\mathcal{B}}^2 \cap \Omega_{\text{play}}$, where $\breve{\mathcal{B}}^2 = \cup_{s=1}^5 \breve{\mathcal{B}}_s^2$ and $\breve{\mathcal{B}}_s^2 = F_s^2(\mathbf{x}_{P_{i1}}^0, \mathbf{x}_{P_{i2}}^0)$ for all $s = 1, \ldots, 5$.

Proof: Since k contains two pursuers P_{i1} and P_{i2}, according to Definition 1, we have $\mathcal{X}_k^0 = \{\mathbf{x}_{P_{i1}}^0, \mathbf{x}_{P_{i2}}^0\}$, $n_k = 2$, and $\mathcal{I}_k = \{m_1, m_2\} = \{i1, i2\}$. Similar to the proof of Theorem 1, ignore the boundary of Ω_{play} and consider $\breve{\mathcal{B}}^2$ first, as shown in Fig. 6(a).

Part (a): It suffices to consider the case where P_{i1} is an active pursuer and P_{i2} is an inactive pursuer.

Since P_{i2} is an inactive pursuer, it follows from Definition 3 that

$$\left\|\mathbf{x}_{P_{i1}}^0 - \boldsymbol{p}\right\|_2 \le \left\|\mathbf{x}_{P_{i2}}^0 - \boldsymbol{p}\right\|_2 \tag{27}$$

holds for all $\boldsymbol{p} \in \mathcal{T}$. Hence, P_{i1} can reach any point in $\mathcal{T}$ no later than P_{i2}, and this feature guarantees that P_{i1} can determine the barrier $\breve{\mathcal{B}}^2$ alone. Thus, $\breve{\mathcal{B}}^2 = \breve{\mathcal{B}}^1(\mathbf{x}_{P_{i1}}^0)$.

Part (b): For two active pursuers case, we will show that $\breve{\mathcal{B}}^2$ includes five parts $\breve{\mathcal{B}}_s^2$ $(s = 1, \ldots, 5)$, as depicted in Fig. 6(a).

Since two pursuers are both active, it follows from Definition 3 that there exist two points $\boldsymbol{p}_1$ and $\boldsymbol{p}_2$ in $\mathcal{T}$ such that

$$\begin{aligned}\left\|\mathbf{x}_{P_{i1}}^0 - \boldsymbol{p}_1\right\|_2 &< \left\|\mathbf{x}_{P_{i2}}^0 - \boldsymbol{p}_1\right\|_2\\ \left\|\mathbf{x}_{P_{i2}}^0 - \boldsymbol{p}_2\right\|_2 &< \left\|\mathbf{x}_{P_{i1}}^0 - \boldsymbol{p}_2\right\|_2.\end{aligned} \tag{28}$$

The former in (28) implies that $\breve{\mathcal{B}}^2$ depends on P_{i1}, and the latter in (28) guarantees that $\breve{\mathcal{B}}^2$ depends on P_{i2}. Thus, in this case, $\breve{\mathcal{B}}^2$ depends on both two pursuers. Naturally, there exists a unique point $\boldsymbol{p}_c = (x_c, 0)$ in $\mathcal{T}$ that two pursuers can reach at the same time, as Fig. 6(a) shows.

Note that in this part, $x_{P_{i1}}^0 \ne x_{P_{i2}}^0$; otherwise, it can be easily verified that one pursuer can reach any point in $\mathcal{T}$ no later than the other, which corresponds to the Part (a). Without loss of generality, assume $x_{P_{i1}}^0 < x_{P_{i2}}^0$ as this theorem states. Thus, $\boldsymbol{p}_c$ is given by

$$\left\|\mathbf{x}_{P_{i1}}^0 - \boldsymbol{p}_c\right\|_2 = \left\|\mathbf{x}_{P_{i2}}^0 - \boldsymbol{p}_c\right\|_2 \Rightarrow x_c = \frac{\left\|\mathbf{x}_{P_{i2}}^0\right\|_2^2 - \left\|\mathbf{x}_{P_{i1}}^0\right\|_2^2}{2(x_{P_{i2}}^0 - x_{P_{i1}}^0)}. \tag{29}$$

If $x_c = 0$, i.e., $\boldsymbol{p}_c = \boldsymbol{m}$, it can be seen from Fig. 6(a) that P_{i2} can reach any point in $\mathcal{T}$ no later than P_{i1}. However, P_{i1} is an active pursuer, so $x_c \ne 0$. Similarly, $x_c \ne l$ can be obtained. Thus, we have $0 < x_c < l$.

Take a point $\boldsymbol{p} = (x_p, 0)$ in $\mathcal{T}$. It can be observed in Fig. 6(a) that if $x_p \in [0, x_c)$, $\|\mathbf{x}_{P_{i1}}^0 - \boldsymbol{p}\|_2 < \|\mathbf{x}_{P_{i2}}^0 - \boldsymbol{p}\|_2$, and if $x_p \in (x_c, l]$, $\|\mathbf{x}_{P_{i2}}^0 - \boldsymbol{p}\|_2 < \|\mathbf{x}_{P_{i1}}^0 - \boldsymbol{p}\|_2$.

Assume E_j can succeed to reach $\mathcal{T}$, and denote E_j's OTP in $\mathcal{T}$ by $\boldsymbol{p}^* = (x_p^*, 0)$ such that J in (11) is maximized. It can be noted that in this case, (11) becomes

$$\begin{aligned}J &= \min_{i=i1,i2} \|\mathbf{x}_{P_i}(t_1) - \mathbf{x}_{E_j}(t_1)\|_2\\ V &= \min_{\mathbf{u}_{P_{i1}}, \mathbf{u}_{P_{i2}} \in \mathcal{U}} \max_{\mathbf{u}_{E_j} \in \mathcal{U}} J\end{aligned} \tag{30}$$

where t_1 is the first arrival time when E_j reaches $\mathcal{T}$. Furthermore, assume $\mathbf{x}_{E_j}^0 \in \breve{\mathcal{B}}^2$. Therefore, under three players' optimal strategies from (30), E_j will be captured exactly when reaching $\mathcal{T}$, namely, $V = 0$.

If $x_p^* \in [0, x_c)$, as Fig. 6(a) shows, this part of $\breve{\mathcal{B}}^2$ is determined by P_{i1} alone, as P_{i1} can reach $\boldsymbol{p}^*$ before P_{i2}. Thus, by following the proof of Theorem 1, it can be obtained that if $x_p^* = 0$, i.e., $\boldsymbol{p}^* = \boldsymbol{m}$, and denote the related barrier by $\breve{\mathcal{B}}_1^2$, then $\breve{\mathcal{B}}_1^2 = \breve{\mathcal{B}}_1^1(\mathbf{x}_{P_{i1}}^0)$, which is the leftmost orange curve in Fig. 6(a) and given by (25) with $\mathbf{x}_{P_i}^0$ replaced by $\mathbf{x}_{P_{i1}}^0$. Thus, it follows from (13) and Theorem 1 that $\breve{\mathcal{B}}_1^2$ can be expressed by a base curve, i.e., $\breve{\mathcal{B}}_1^2 = F_1^2(\mathbf{x}_{P_{i1}}^0, \mathbf{x}_{P_{i2}}^0)$.

Consider the remainder $x_p^* \in (0, x_c)$ and denote the related barrier by $\breve{\mathcal{B}}_2^2$, which is the leftmost black curve in Fig. 6(a). Next, we compute the expression of $\breve{\mathcal{B}}_2^2$.

Since $x_p^* \in (0, x_c)$ and J in (30) only depends on P_{i1}, it follows from the proof of Theorem 1 that (20) and (21) still

hold for P_{i1} and E_j, that is, $x_p^* = \frac{x_{E_j}^0 - \alpha^2 x_{P_{i1}}^0}{1-\alpha^2}$ and

$$\left(x_{E_j}^0 - x_{P_{i1}}^0\right)^2 + \left(1 - 1/\alpha^2\right)\left(y_{E_j}^0\right)^2 + \left(1-\alpha^2\right)\left(y_{P_{i1}}^0\right)^2 = 0 \tag{31}$$

representing the relationship between the initial positions of P_{i1} and E_j when $\mathbf{x}_{E_j}^0 \in \breve{\mathcal{B}}_2^2$. From $x_p^* \in (0, x_c)$, we have

$$x_{E_j}^0 \in \left(\alpha^2 x_{P_{i1}}^0, (1-\alpha^2)x_c + \alpha^2 x_{P_{i1}}^0\right). \tag{32}$$

Hence, by replacing $\mathbf{x}_{E_j}^0$ with a general variable $\mathbf{z} \in \mathbb{R}^2$, it follows from (31), (32) and $y_{E_j}^0 < 0$ that $\breve{\mathcal{B}}_2^2$ is as follows:

$$\begin{aligned}\breve{\mathcal{B}}_2^2 = \big\{\mathbf{z} = (x,y) \in \mathbb{R}^2 | &\left(x - x_{P_{i1}}^0\right)^2 + \left(1 - 1/\alpha^2\right)y^2 \\ &+ (1-\alpha^2)\left(y_{P_{i1}}^0\right)^2 = 0, x \in (k_3, k_4), \quad y < 0\big\}\end{aligned} \tag{33}$$

where $k_3 = \alpha^2 x_{P_{i1}}^0$ and $k_4 = (1-\alpha^2)x_c + \alpha^2 x_{P_{i1}}^0$. For clarity, it can be seen that $\breve{\mathcal{B}}_2^2$ can be expressed by a base curve in (13), that is, $\breve{\mathcal{B}}_2^2 = F_2^2(\mathbf{x}_{P_{i1}}^0, \mathbf{x}_{P_{i2}}^0)$.

Analogously, when P_{i2} can reach $\boldsymbol{p}^*$ before P_{i1}, i.e., $x_p^* \in (x_c, l]$, as Fig. 6(a) shows, $\breve{\mathcal{B}}_4^2 = F_4^2(\mathbf{x}_{P_{i1}}^0, \mathbf{x}_{P_{i2}}^0)$ and $\breve{\mathcal{B}}_5^2 = F_5^2(\mathbf{x}_{P_{i1}}^0, \mathbf{x}_{P_{i2}}^0)$ can be derived respectively for $x_p^* \in (x_c, l)$ and $x_p^* = l$, where $\breve{\mathcal{B}}_4^2$ is the rightmost black curve and $\breve{\mathcal{B}}_5^2$ is the rightmost orange curve.

Finally, consider the case $x_p^* = x_c$, i.e., $\boldsymbol{p}^* = \boldsymbol{p}_c$, which corresponds to the middle orange barrier $\breve{\mathcal{B}}_3^2$ in Fig. 6(a). Note that (19) still holds for P_{i1} and E_j and can be rewritten as

$$\left\|\boldsymbol{p}_c - \mathbf{x}_{E_j}^0\right\|_2 = \alpha\left\|\boldsymbol{p}_c - \mathbf{x}_{P_{i1}}^0\right\|_2. \tag{34}$$

Naturally, $x_{E_j}^0$ should lie in $[k_4, k_5]$, where $k_5 = (1-\alpha^2)x_c + \alpha^2 x_{P_{i2}}^0$ which actually is the boundary of the x value of $\breve{\mathcal{B}}_4^2$. Thus, by replacing $\mathbf{x}_{E_j}^0$ with a general variable $\mathbf{z} \in \mathbb{R}^2$, it follows from (34) and $y_{E_j}^0 < 0$ that $\breve{\mathcal{B}}_3^2$ is as follows:

$$\begin{aligned}\breve{\mathcal{B}}_3^2 = \big\{\mathbf{z} = (x,y) \in \mathbb{R}^2 \big| &\left\|\mathbf{z} - \boldsymbol{p}_c\right\|_2 \\ &= \alpha\left\|\mathbf{x}_{P_{i1}}^0 - \boldsymbol{p}_c\right\|_2, x \in [k_4, k_5], \quad y < 0\big\}.\end{aligned} \tag{35}$$

It can also be noted that $\breve{\mathcal{B}}_3^2$ can be expressed by a base curve in (13), that is, $\breve{\mathcal{B}}_3^2 = F_3^2(\mathbf{x}_{P_{i1}}^0, \mathbf{x}_{P_{i2}}^0)$.

Therefore, we have constructed the barrier $\breve{\mathcal{B}}^2 = \cup_{s=1}^5 \breve{\mathcal{B}}_s^2$, without considering the boundary of Ω_{play}, shown in Fig. 6(a). Now, consider the effect of the boundary of Ω_{play}. Since the optimal trajectories for three players (if it works in the payoff function J) are straight lines and Ω_{play} is convex, $\mathcal{B}^2 = \breve{\mathcal{B}}^2 \cap \Omega_{\text{play}}$ holds, as Fig. 6(b) shows. Intuitively, the PWR $\mathcal{W}_P^2$ is the green region, and the EWR $\mathcal{W}_E^2$ is the red region. □

D. General Pursuit Coalitions Versus One Evader

The objective in this section is to construct the barrier for general pursuit coalitions with the inspiration from the results derived in two pursuers case. First, the barrier for a special class of pursuit coalitions whose pursuers are all active, is constructed. Then theoretically, it is demonstrated that every pursuit coalition can be degenerated into a unique pursuit subcoalition of this class. Finally, this pursuit subcoalition and the original pursuit coalition are proved to possess the same barrier. To this end, the definition of this special class pursuit coalition is formally introduced as follows.

Definition 6 (Full-Active Pursuit Coalition): Given a pursuit coalition k, if for any pursuer P_i ($i \in \mathcal{I}_k$) in k, there always exists a point in $\mathcal{T}$ that P_i can reach before all other pursuers in k, then k is called a full-active pursuit coalition.

It can be verified that if a pursuit coalition k is full-active, its members must have different x-coordinates. Otherwise, assume that in k, P_{i1}, and P_{i2} have the same x-coordinate. Thus, it can be noted that one pursuer can reach any point in $\mathcal{T}$ no later than the other one, which contradicts with the fact that two pursuers are both active. Hence, for every full-active pursuit coalition k with $n_k \geq 2$, introduce an auxiliary index set $\hat{\mathcal{I}}_k = \{\hat{m}_j | 1 \leq \hat{m}_j \leq N_p, j = 1, 2, \ldots, n_k\} = \mathcal{I}_k$ such that $x_{P_{\hat{m}_i}}^0 < x_{P_{\hat{m}_{i+1}}}^0$ holds for all $i = 1, 2, \ldots, n_k - 1$. More intuitively, we mean that $P_{\hat{m}_i}$ lies at the left side of $P_{\hat{m}_{i+1}}$ along the x-axis. We call $\hat{\mathcal{I}}_k$ as x-rank index set, and obviously it is unique.

With the above x-rank index set $\hat{\mathcal{I}}_k$, the theorem presented as follows provides a scheme to construct the barrier for full-active pursuit coalitions.

Theorem 3 (Barrier for Full-Active Pursuit Coalition): Consider the system (1) and suppose that Assumptions 1, 2, and 4 hold. If a pursuit coalition k with the initial condition $\mathcal{X}_k^0$ and n_k pursuers, is full-active, its corresponding barrier can be constructed analytically as follows:

i) If $n_k = 1$, $\mathcal{B}^{n_k}(\mathcal{X}_k^0)$ is given by Theorem 1. If $n_k = 2$, $\mathcal{B}^{n_k}(\mathcal{X}_k^0)$ is given by Theorem 2(b).

ii) If $3 \leq n_k \leq N_p$, let $\hat{\mathcal{I}}_k$ denote its x-rank index set. Then, $\mathcal{B}^{n_k}(\mathcal{X}_k^0) = \breve{\mathcal{B}}^{n_k} \cap \Omega_{\text{play}}$, where

$$\begin{aligned}\breve{\mathcal{B}}^{n_k} = &\cup_{i=1}^2 F_i^2\left(\mathbf{x}_{P_{\hat{m}_1}}^0, \mathbf{x}_{P_{\hat{m}_2}}^0\right) \cup_{i=1}^{n_k-1} F_3^2\left(\mathbf{x}_{P_{\hat{m}_i}}^0, \mathbf{x}_{P_{\hat{m}_{i+1}}}^0\right) \\ &\times \cup_{i=2}^{n_k-1} F^3\left(\mathbf{x}_{P_{\hat{m}_{i-1}}}^0, \mathbf{x}_{P_{\hat{m}_i}}^0, \mathbf{x}_{P_{\hat{m}_{i+1}}}^0\right) \\ &\times \cup_{i=4}^5 F_i^2\left(\mathbf{x}_{P_{\hat{m}_{n_k-1}}}^0, \mathbf{x}_{P_{\hat{m}_{n_k}}}^0\right).\end{aligned} \tag{36}$$

Proof: Note that the conclusion (i) is straightforward. Thus, we focus on the conclusion (ii). Construct $\breve{\mathcal{B}}^{n_k}$ first, namely, ignore the boundary of Ω_{play}.

Since k is full-active, according to Definition 6, for every pursuer in k, there always exists a point in $\mathcal{T}$ that it can reach before all other pursuers in k. Thus, every pursuer in k contributes to $\breve{\mathcal{B}}^{n_k}$.

Next, a method is presented to construct the barrier $\breve{\mathcal{B}}^{n_k}$. First, by Theorem 2(b), construct the barrier $\breve{\mathcal{B}}^2$ determined by $P_{\hat{m}_1}$ and $P_{\hat{m}_2}$, as Fig. 6(a) shows by replacing P_{i1} and P_{i2} with $P_{\hat{m}_1}$ and $P_{\hat{m}_2}$ respectively. Then, add the third pursuer $P_{\hat{m}_3}$ and compute the associated $\breve{\mathcal{B}}^3$ which is proved as follows to consist of seven parts, as Fig. 7(a) shows.

According to the definition of the x-rank index set presented above, $x_{P_{\hat{m}_1}}^0 < x_{P_{\hat{m}_2}}^0 < x_{P_{\hat{m}_3}}^0$ holds. Take two points $\boldsymbol{p}_{c1}$ and $\boldsymbol{p}_{c2}$ in $\mathcal{T}$ such that

$$\left\|\mathbf{x}_{P_{\hat{m}_i}}^0 - \boldsymbol{p}_{ci}\right\|_2 = \left\|\mathbf{x}_{P_{\hat{m}_{i+1}}}^0 - \boldsymbol{p}_{ci}\right\|_2, \quad i = 1, 2 \tag{37}$$

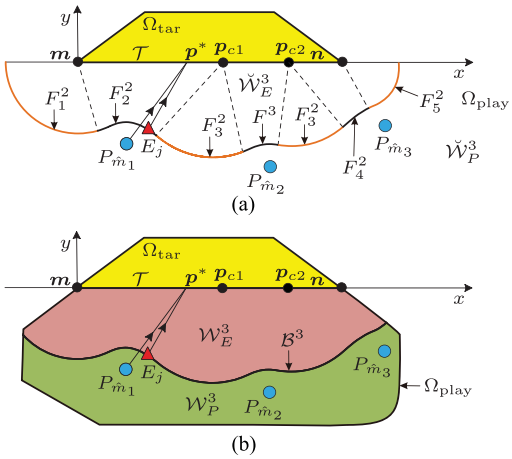

Fig. 7. Barrier and two winning regions determined by three active pursuers $P_{\hat{m}_1}, P_{\hat{m}_2}$, and $P_{\hat{m}_3}$ when playing with E_j, in which all three pursuers contribute to the construction of $\breve{\mathcal{B}}^3$. (a) Without considering the boundary of Ω_{play}, the barrier $\breve{\mathcal{B}}^3$ consists of seven parts. Two winning regions $\breve{\mathcal{W}}_P^3$ and $\breve{\mathcal{W}}_E^3$ for each team's guaranteed winning are split by $\breve{\mathcal{B}}^3$. (b) By considering the boundary of Ω_{play}, $\mathcal{B}^3$ is given by $\breve{\mathcal{B}}^3 \cap \Omega_{\text{play}}$, as the optimal trajectories for the players who work in the payoff function, are straight lines and Ω_{play} is convex. Naturally, $\breve{\mathcal{W}}_P^3$ becomes the green region $\mathcal{W}_P^3$, and $\breve{\mathcal{W}}_E^3$ becomes the red region $\mathcal{W}_E^3$.

holds, as depicted in Fig. 7(a), that is, $\boldsymbol{p}_{ci}$ is the point in $\mathcal{T}$ having the same distance to $P_{\hat{m}_i}$ and $P_{\hat{m}_{i+1}}$. Thus, from (37), $\boldsymbol{p}_{ci} = (x_{ci}, 0)$ can be computed as follows:

$$x_{ci} = \frac{\left\|\mathbf{x}^0_{P_{\hat{m}_{i+1}}}\right\|_2^2 - \left\|\mathbf{x}^0_{P_{\hat{m}_i}}\right\|_2^2}{2\left(x^0_{P_{\hat{m}_{i+1}}} - x^0_{P_{\hat{m}_i}}\right)}, \quad i = 1, 2. \tag{38}$$

Since $P_{\hat{m}_1}$ is an active pursuer, there must exist a point in $\mathcal{T}$ that $P_{\hat{m}_1}$ can reach before $P_{\hat{m}_2}$. Thus, $x_{c1} > 0$, as Fig. 7(a) shows. Similarly, $x_{c2} < l$ also holds. Take a point $\boldsymbol{p} = (x_p, 0)$ in $\mathcal{T}$. It can be obtained that if $x_p \in [0, x_{c1})$, $P_{\hat{m}_1}$ can reach $\boldsymbol{p}$ before $P_{\hat{m}_2}$, and if $x_p \in (x_{c2}, l]$, $P_{\hat{m}_3}$ can reach $\boldsymbol{p}$ before $P_{\hat{m}_2}$. Since $P_{\hat{m}_2}$ is an active pursuer, there must exist a point in $\mathcal{T}$ that $P_{\hat{m}_2}$ can reach before both $P_{\hat{m}_1}$ and $P_{\hat{m}_3}$. Thus, $x_{c1} < x_{c2}$ holds. In conclusion, $0 < x_{c1} < x_{c2} < l$ is derived, as Fig. 7(a) illustrates.

Assume E_j can succeed to reach $\mathcal{T}$, and denote E_j's OTP in $\mathcal{T}$ by $\boldsymbol{p}^* = (x_p^*, 0)$ such that J in (11) only involving these three pursuers is maximized. Thus in this case, (11) becomes

$$\begin{aligned} J &= \min_{i=\hat{m}_1,\hat{m}_2,\hat{m}_3} \|\mathbf{x}_{P_i}(t_1) - \mathbf{x}_{E_j}(t_1)\|_2 \\ V &= \min_{\mathbf{u}_{P_{\hat{m}_1}},\mathbf{u}_{P_{\hat{m}_2}},\mathbf{u}_{P_{\hat{m}_3}} \in \mathcal{U}} \max_{\mathbf{u}_{E_j} \in \mathcal{U}} J \end{aligned} \tag{39}$$

where t_1 is the first arrival time when E_j reaches $\mathcal{T}$. Similarly, we further assume $\mathbf{x}^0_{E_j} \in \breve{\mathcal{B}}^3$. Therefore, under four players' optimal strategies from (39), E_j will be captured exactly when reaching $\mathcal{T}$, namely, $V = 0$.

If $x_p^* \in [0, x_{c1})$, as Fig. 7(a) shows, $P_{\hat{m}_1}$ can reach $\boldsymbol{p}^*$ before both $P_{\hat{m}_2}$ and $P_{\hat{m}_3}$. Thus, this part of $\breve{\mathcal{B}}^3$ is determined by $P_{\hat{m}_1}$ alone, namely, J only depends on $P_{\hat{m}_1}$. By following the proof of Theorem 2, the part related to $P_{\hat{m}_1}$ alone is given by $F_1^2(\mathbf{x}^0_{P_{\hat{m}_1}}, \mathbf{x}^0_{P_{\hat{m}_2}}) \cup F_2^2(\mathbf{x}^0_{P_{\hat{m}_1}}, \mathbf{x}^0_{P_{\hat{m}_2}})$, respectively for $x_p^* = 0$ and $x_p^* \in (0, x_{c1})$, which consists of the leftmost orange and black curves in Fig. 7(a).

If $x_p^* \in (x_{c1}, x_{c2})$, as Fig. 7(a) shows, $P_{\hat{m}_2}$ can reach $\boldsymbol{p}^*$ before both $P_{\hat{m}_1}$ and $P_{\hat{m}_3}$, implying that this part of $\breve{\mathcal{B}}^3$ is determined by $P_{\hat{m}_2}$ alone, namely, J only depends on $P_{\hat{m}_2}$. Thus, it follows from the proof of Theorem 1 that (20) and (21) hold for $P_{\hat{m}_2}$ and E_j, that is, $x_p^* = \frac{x^0_{E_j} - \alpha^2 x^0_{P_{\hat{m}_2}}}{1-\alpha^2}$ and:

$$\left(x^0_{E_j} - x^0_{P_{\hat{m}_2}}\right)^2 + \left(1 - 1/\alpha^2\right)\left(y^0_{E_j}\right)^2 + (1-\alpha^2)\left(y^0_{P_{\hat{m}_2}}\right)^2 = 0 \tag{40}$$

which characterizes the relationship between the initial positions of $P_{\hat{m}_2}$ and E_j when $\mathbf{x}^0_{E_j} \in \breve{\mathcal{B}}^3$ and $x_p^* \in (x_{c1}, x_{c2})$. Also note that from $x_p^* \in (x_{c1}, x_{c2})$, we have

$$x^0_{E_j} \in \left((1-\alpha^2)x_{c1} + \alpha^2 x^0_{P_{\hat{m}_2}}, (1-\alpha^2)x_{c2} + \alpha^2 x^0_{P_{\hat{m}_2}}\right). \tag{41}$$

Therefore, by replacing $\mathbf{x}^0_{E_j}$ with a general variable $\mathbf{z} \in \mathbb{R}^2$, it follows from (40), (41) and $y^0_{E_j} < 0$ that this part of $\breve{\mathcal{B}}^3$, which is the middle black curve in Fig. 7(a), is given by

$$\begin{aligned} \Big\{\mathbf{z} = (x, y) \in \mathbb{R}^2 \Big| &\left(x - x^0_{P_{\hat{m}_2}}\right)^2 + (1 - 1/\alpha^2)y^2 \\ &+ (1-\alpha^2)\left(y^0_{P_{\hat{m}_2}}\right)^2 = 0, x \in (k_7, k_8), y < 0\Big\} \end{aligned} \tag{42}$$

where $k_7 = (1-\alpha^2)x_{c1} + \alpha^2 x^0_{P_{\hat{m}_2}}$ and $k_8 = (1-\alpha^2)x_{c2} + \alpha^2 x^0_{P_{\hat{m}_2}}$. From (14), it can be noted that (42) can be expressed by a base curve, that is, $F^3(\mathbf{x}^0_{P_{\hat{m}_1}}, \mathbf{x}^0_{P_{\hat{m}_2}}, \mathbf{x}^0_{P_{\hat{m}_3}})$.

If $x_p^* \in (x_{c2}, l]$, as Fig. 7(a) shows, this part of $\breve{\mathcal{B}}^3$ is only related to $P_{\hat{m}_3}$. Based on the similar analysis for the case $x_p^* \in [0, x_{c1})$, this part, which consists of the rightmost black and orange curves in Fig. 7(a), is given by $F_4^2(\mathbf{x}^0_{P_{\hat{m}_2}}, \mathbf{x}^0_{P_{\hat{m}_3}}) \cup F_5^2(\mathbf{x}^0_{P_{\hat{m}_2}}, \mathbf{x}^0_{P_{\hat{m}_3}})$.

Now, we consider the remainder $x_p^* = x_{c1}$ or $x_p^* = x_{c2}$. For simplicity, we only consider $x_p^* = x_{c1}$, and similar analysis can be conducted for $x_p^* = x_{c2}$. Note that $x_p^* = x_{c1}$, i.e., $\boldsymbol{p}^* = \boldsymbol{p}_{c1}$, and (19) holds for $P_{\hat{m}_1}$ and E_j. Similar to the analysis for $x_p^* = x_c$ in the proof of Theorem 2, this part of $\breve{\mathcal{B}}^3$, which is the second orange curve from the left in Fig. 7(a), is given by a base curve in (13), that is, $F_3^2(\mathbf{x}^0_{P_{\hat{m}_1}}, \mathbf{x}^0_{P_{\hat{m}_2}})$.

Thus, by connecting all these parts of $\breve{\mathcal{B}}^3$, we can obtain $\breve{\mathcal{B}}^3$ given by (36) with $n_k = 3$, shown in Fig. 7(a).

Similarly, add the fourth pursuer $P_{\hat{m}_4}$, and $\boldsymbol{p}_{c3} = (x_{c3}, 0)$ is given by (38) with $i = 3$. Then, $0 < x_{c1} < x_{c2} < x_{c3} < l$ can be obtained. In the same way, $\breve{\mathcal{B}}^4$ is given by (36) with $n_k = 4$. Therefore, by adding the remaining pursuers one-by-one along the x-rank index set $\hat{\mathcal{I}}_k$, $\breve{\mathcal{B}}^{n_k}$ is obtained as (36) shows.

Then, consider the effect of the boundary of Ω_{play}. Since the optimal trajectories for the players who work in the payoff function J, are straight lines and Ω_{play} is convex, it can be obtained that $\mathcal{B}^{n_k} = \breve{\mathcal{B}}^{n_k} \cap \Omega_{\text{play}}$, as Fig. 7(b) shows when

$n_k = 3$. Naturally, the PWR $\mathcal{W}_P^3$ is the green region, and the EWR $\mathcal{W}_E^3$ is the red region. Thus we finish the proof. □

Note that in general pursuit coalitions, there may exist some inactive pursuers who as asserted as follows, have no effect on the barrier construction but instead hinder our analysis. In light of this, if all active pursuers can be extracted out from any given pursuit coalition, namely, its largest full-active pursuit subcoalition, then the barrier for this general pursuit coalition can be obtained from Theorem 3.

First, the following lemma formally establishes a connection of the barrier between a general pursuit coalition and its largest full-active pursuit subcoalition.

Lemma 3 (Barrier Equivalence): For any pursuit coalition k, $\mathcal{B}^{n_k}(\mathcal{X}_k^0) = \mathcal{B}^{\bar{n}_k}(\bar{\mathcal{X}}_k^0)$ holds, where $\bar{\mathcal{X}}_k^0$ with $\bar{n}_k$ pursuers denotes the initial position of the unique largest full-active pursuit subcoalition of $\mathcal{X}_k^0$.

Proof: Obviously, we only need to focus on the case that $\mathcal{X}_k^0 \setminus \bar{\mathcal{X}}_k^0$ is nonempty. Thus, $n_k > \bar{n}_k$. For simplicity, we prove $\mathcal{W}_E^{n_k} = \mathcal{W}_E^{\bar{n}_k}$. By definition, $\mathcal{W}_E^{n_k} \subseteq \mathcal{W}_E^{\bar{n}_k}$ holds, as reducing the pursuer will result in the same or expansion of the EWR. Thus we only need to verify $\mathcal{W}_E^{\bar{n}_k} \subseteq \mathcal{W}_E^{n_k}$, equivalently, $\breve{\mathcal{W}}_E^{\bar{n}_k} \subseteq \breve{\mathcal{W}}_E^{n_k}$.

Suppose $\boldsymbol{p} \in \breve{\mathcal{W}}_E^{\bar{n}_k}$. Then, there must exist a point $\boldsymbol{p}_1 \in \mathcal{T}$ such that

$$\|\boldsymbol{p} - \boldsymbol{p}_1\|_2 < \alpha \left\|\mathbf{x}_{P_i}^0 - \boldsymbol{p}_1\right\|_2 \tag{43}$$

holds for all $\mathbf{x}_{P_i}^0 \in \bar{\mathcal{X}}_k^0$. Assume that there exists a pursuer P_j satisfying $\mathbf{x}_{P_j}^0 \in \mathcal{X}_k^0 \setminus \bar{\mathcal{X}}_k^0$ and

$$\alpha \left\|\mathbf{x}_{P_j}^0 - \boldsymbol{p}_1\right\|_2 \le \left\|\boldsymbol{p} - \boldsymbol{p}_1\right\|_2 \tag{44}$$

Then, by (43) and (44), it can be stated that

$$\left\|\mathbf{x}_{P_j}^0 - \boldsymbol{p}_1\right\|_2 < \left\|\mathbf{x}_{P_i}^0 - \boldsymbol{p}_1\right\|_2 \tag{45}$$

holds for all $\mathbf{x}_{P_i}^0 \in \bar{\mathcal{X}}_k^0$. Thus, there exists a point, i.e, $\boldsymbol{p}_1$, in $\mathcal{T}$ that P_j can reach before all pursuers in $\bar{\mathcal{X}}_k^0$, which contradicts with the fact that $\bar{\mathcal{X}}_k^0$ is the largest full-active pursuit subcoalition of $\mathcal{X}_k^0$. Therefore, we can conclude that (44) does not hold, that is

$$\|\boldsymbol{p} - \boldsymbol{p}_1\|_2 < \alpha \left\|\mathbf{x}_{P_j}^0 - \boldsymbol{p}_1\right\|_2 \tag{46}$$

holds for all $\mathbf{x}_{P_j}^0 \in \mathcal{X}_k^0 \setminus \bar{\mathcal{X}}_k^0$. Combining (43) with (46) shows that there exists a point, i.e., $\boldsymbol{p}_1$, in $\mathcal{T}$ that $\boldsymbol{p}$ can reach before all pursuers in $\mathcal{X}_k^0$ with a speed ratio α. Thus, $\boldsymbol{p} \in \breve{\mathcal{W}}_E^{n_k}$, implying that $\breve{\mathcal{W}}_E^{\bar{n}_k} \subseteq \breve{\mathcal{W}}_E^{n_k}$.

The existence of $\bar{\mathcal{X}}_k^0$ is straightforward, as $\bar{\mathcal{X}}_k^0$ is a subset of $\mathcal{X}_k^0$. As for the uniqueness, assume that $\bar{\mathcal{X}}_k^0$ with $\bar{n}_k$ pursuers and $\bar{\mathcal{Y}}_k^0$ with $\bar{m}_k$ pursuers are two distinct largest full-active pursuit subcoalitions of $\mathcal{X}_k^0$.

Take a pursuer P_i satisfying $\mathbf{x}_{P_i}^0 \in \bar{\mathcal{X}}_k^0$ and $\mathbf{x}_{P_i}^0 \notin \bar{\mathcal{Y}}_k^0$. Then, it follows from Definition 6 that $\mathbf{x}_{P_i}^0 \notin \bar{\mathcal{Y}}_k^0$ implies that there is no point in $\mathcal{T}$ that P_i can reach before all pursuers in $\bar{\mathcal{Y}}_k^0$. In other words, there is no point in $\mathcal{T}$ that P_i can reach before all other pursuers in $\mathcal{X}_k^0$, which contradicts with the fact that $\mathbf{x}_{P_i}^0$ is an active pursuer by noting that $\mathbf{x}_{P_i}^0 \in \bar{\mathcal{X}}_k^0$. Thus, $\bar{\mathcal{X}}_k^0 = \bar{\mathcal{Y}}_k^0$ and the uniqueness is proved. □

Algorithm 1: (Algorithm for Finding the Largest Full-Active Pursuit Subcoalition in k).

1: **Input:** $\mathcal{X}_k^0 \in \Omega_{\text{play}}^{n_k} \cup \mathcal{T}^{n_k}, \bar{\mathcal{X}}_k^0 \leftarrow \emptyset, \bar{n}_k \leftarrow 0$.
2: **for** $i \in \{1, \ldots, n_k\}$ **do**
3: $\quad \mathcal{T}_1 = \mathcal{T}$
4: $\quad$ **for** $j \in \{1, \ldots, n_k\}, j \neq i$ **do**
5: $\quad\quad \mathcal{T}_1 = \mathcal{R}_D(\mathbf{x}_{P_{m_i}}^0, \mathbf{x}_{P_{m_j}}^0) \cap \mathcal{T}_1$
6: $\quad$ **end for**
7: $\quad$ **if** $\mathcal{T}_1 \neq \emptyset$ **then**
8: $\quad\quad \bar{\mathcal{X}}_k^0 \leftarrow \bar{\mathcal{X}}_k^0 \cup \mathbf{x}_{P_{m_i}}^0, \bar{n}_k \leftarrow \bar{n}_k + 1$
9: $\quad$ **end if**
10: **end for**
11: **Output:** $\bar{\mathcal{X}}_k^0, \bar{n}_k$.

Denote by $\mathcal{R}_D$ the set of points in $\mathbb{R}^2$ that P_{m_i} can reach before P_{m_j}, which is mathematically formulated as follows:

$$\mathcal{R}_D\left(\mathbf{x}_{P_{m_i}}^0, \mathbf{x}_{P_{m_j}}^0\right) = \left\{\mathbf{z} \in \mathbb{R}^2 \middle| \left\|\mathbf{z} - \mathbf{x}_{P_{m_i}}^0\right\|_2 < \left\|\mathbf{z} - \mathbf{x}_{P_{m_j}}^0\right\|_2\right\}. \tag{47}$$

It can be noted that $\mathcal{R}_D$ is a half plane.

Next, for a pursuit coalition k, an algorithm is presented to find its unique largest full-active pursuit subcoalition, namely, $\bar{\mathcal{X}}_k^0$. To avoid redundant illustration, the proof of this algorithm is left in the next theorem.

Now it suffices to present the main result of this section.

Theorem 4 (Barrier for General Pursuit Coalition): Consider the system (1) satisfying Assumptions 1, 2, and 4. For a pursuit coalition k, its largest full-active pursuit subcoalition $\bar{\mathcal{X}}_k^0$ with $\bar{n}_k$ pursuers can be found by Algorithm 1. Then, $\mathcal{B}^{n_k}(\mathcal{X}_k^0) = \mathcal{B}^{\bar{n}_k}(\bar{\mathcal{X}}_k^0)$, where $\mathcal{B}^{\bar{n}_k}(\bar{\mathcal{X}}_k^0)$ can be computed by Theorem 3.

Proof: According to Lemma 3 and Theorem 3, if the validity of Algorithm 1 can be verified, this theorem holds naturally.

From line 3 to line 6 in Algorithm 1, the set of points in $\mathcal{T}$ that P_{m_i} can reach before all other pursuers in k, is computed and denoted by $\mathcal{T}_1$, where $\mathcal{R}_D(\mathbf{x}_{P_{m_i}}^0, \mathbf{x}_{P_{m_j}}^0)$ denotes the set of points in $\mathbb{R}^2$ that P_{m_i} can reach before P_{m_j} as shown in (47). Thus, if $\mathcal{T}_1 \neq \emptyset$, that is, there exists at least one point that P_i can reach before all other pursuers in k, then P_i must be an active pursuer in k. Conversely, if $\mathcal{T}_1 = \emptyset$, namely, there is no point in $\mathcal{T}$ that P_i can reach before all other pursuers in k, then P_i must be an inactive pursuer in k. □

E. Extensions to Relaxed Initial Deployment

In this section, the barrier construction method will be extended to the scenarios having more realistic initial deployment as Assumption 3 shows. In this initial deployment, pursuers are allowed to initially lie in Ω_{tar}. For example, there may exist pursuers who are patrolling in Ω_{tar} exactly when evaders are

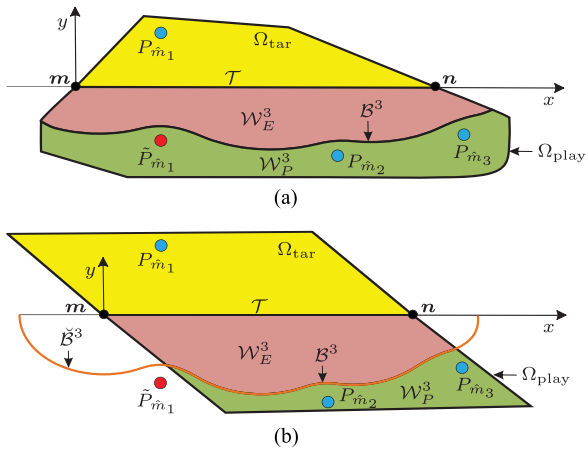

Fig. 8. Barrier and winning regions for relaxed initial deployment which allows the pursuer to start the game from Ω_{tar}. The red circle $\tilde{P}_{\hat{m}_1}$ is the virtual pursuer of $P_{\hat{m}_1}$, and they are symmetric with respect to $\mathcal{T}$. It is proved that the barrier $\mathcal{B}^3$ determined by $P_{\hat{m}_1}, P_{\hat{m}_2}$, and $P_{\hat{m}_3}$ is the same as the barrier determined by $\tilde{P}_{\hat{m}_1}, P_{\hat{m}_2}$, and $P_{\hat{m}_3}$. This feature is called mirror property. (a) $\tilde{P}_{\hat{m}_1}$ lies in Ω; (b) $\tilde{P}_{\hat{m}_1}$ lies out of Ω.

detected. As discussed in the following, by introducing a specific virtual pursuer, a road between this case and the known results is established. Or, more concretely, it is demonstrated that this virtual pursuer plays the same role with its original pursuer in barrier construction.

Definition 7 (Virtual Pursuer): For every pursuer P_i whose initial condition satisfies $\mathbf{x}_{P_i}^0 = (x_{P_i}^0, y_{P_i}^0) \in \Omega_{\text{tar}}$, introduce a virtual pursuer $\tilde{P}_i$ with the initial position $\tilde{\mathbf{x}}_{P_i}^0 = (\tilde{x}_{P_i}^0, \tilde{y}_{P_i}^0)$ such that $\tilde{x}_{P_i}^0 = x_{P_i}^0$ and $\tilde{y}_{P_i}^0 = -y_{P_i}^0$.

Remark 3: It can be easily observed that the virtual pursuer and its original pursuer are symmetric with respect to $\mathcal{T}$, and a three-pursuer pursuit coalition example is presented in Fig. 8 where $P_{\hat{m}_1}$ lies in Ω_{tar} and its virtual pursuer is the red circle $\tilde{P}_{\hat{m}_1}$. Since Ω_{play} and Ω_{tar} allow different shapes, the virtual pursuer may lie in or out of Ω, as Fig. 8(a) and (b) indicate that $\tilde{P}_{\hat{m}_1}$ lies in or out of Ω.

Note that the virtual pursuer generated by one pursuer may coincide with another pursuer, which will lead to a disagreement with Assumption 1. Thus, an assumption on the virtual pursuer is as follows.

Assumption 5: Assume that every virtual pursuer does not coincide with all other pursuers. However, the coincidence of the virtual pursuer and its own original pursuer is allowed, namely, when $\mathbf{x}_{P_i}^0 \in \mathcal{T}$.

Next, an important property of virtual pursuers in terms of the barrier construction will be stated, which is a key step to simplify the problems.

Lemma 4 (Mirror Property): For k, if $\mathbf{x}_{P_i}^0 \in \Omega_{\text{tar}}$ $(i \in \mathcal{I}_k)$, let $\mathcal{X}_k^0(-i)$ denote the rest of pursuers in k when $\mathbf{x}_{P_i}^0$ is removed, and $\tilde{\mathbf{x}}_{P_i}^0$ denote the virtual pursuer of $\mathbf{x}_{P_i}^0$. Then, $\mathcal{B}^{n_k}(\mathcal{X}_k^0) = \mathcal{B}^{n_k}(\mathcal{X}_k^0(-i) \cup \tilde{\mathbf{x}}_{P_i}^0)$.

Proof: Suppose $\boldsymbol{p} \in \mathcal{W}_E^{n_k}(\mathcal{X}_k^0(-i) \cup \tilde{\mathbf{x}}_{P_i}^0)$, and then there must exist a point $\boldsymbol{p}_1 \in \mathcal{T}$ such that

$$\|\boldsymbol{p} - \boldsymbol{p}_1\|_2 < \alpha \left\|\mathbf{x}_{P_j}^0 - \boldsymbol{p}_1\right\|_2 \tag{48}$$

holds for all $\mathbf{x}_{P_j}^0 \in \mathcal{X}_k^0(-i) \cup \tilde{\mathbf{x}}_{P_i}^0$. According to Definition 7, we have

$$\left\|\mathbf{x}_{P_i}^0 - \boldsymbol{p}_1\right\|_2 = \left\|\tilde{\mathbf{x}}_{P_i}^0 - \boldsymbol{p}_1\right\|_2. \tag{49}$$

Naturally, (48) holds for all $\mathbf{x}_{P_j}^0 \in \mathcal{X}_k^0$, which implies that $\boldsymbol{p} \in \mathcal{W}_E^{n_k}(\mathcal{X}_k^0)$. Therefore, $\mathcal{W}_E^{n_k}(\mathcal{X}_k^0(-i) \cup \tilde{\mathbf{x}}_{P_i}^0) \subset \mathcal{W}_E^{n_k}(\mathcal{X}_k^0)$ is obtained.

On the other side, suppose $\boldsymbol{p} \in \mathcal{W}_E^{n_k}(\mathcal{X}_k^0)$ and in the similar way, $\boldsymbol{p} \in \mathcal{W}_E^{n_k}(\mathcal{X}_k^0(-i) \cup \tilde{\mathbf{x}}_{P_i}^0)$ can be derived, implying $\mathcal{W}_E^{n_k}(\mathcal{X}_k^0) \subset \mathcal{W}_E^{n_k}(\mathcal{X}_k^0(-i) \cup \tilde{\mathbf{x}}_{P_i}^0)$. Thus, $\mathcal{W}_E^{n_k}(\mathcal{X}_k^0) = \mathcal{W}_E^{n_k}(\mathcal{X}_k^0(-i) \cup \tilde{\mathbf{x}}_{P_i}^0)$, which finishes the proof by noting that $\mathcal{B}^{n_k}$ is the separating curve between $\mathcal{W}_P^{n_k}$ and $\mathcal{W}_E^{n_k}$.

A three pursuer case is presented in Fig. 8, where $P_{\hat{m}_1}$ lies in Ω_{tar}. If $\tilde{P}_{\hat{m}_1}$ lies in Ω as Fig. 8(a) shows, the correctness of the mirror property is straightforward as proved above. If $\tilde{P}_{\hat{m}_1}$ lies out of Ω as Fig. 8(b) shows, we can still first construct the barrier $\check{\mathcal{B}}^3$ (orange) by $\tilde{P}_{\hat{m}_1}, P_{\hat{m}_2}$, and $P_{\hat{m}_3}$, and then compute $\mathcal{B}^3$ which is the intersection set $\check{\mathcal{B}}^3 \cap \Omega_{\text{play}}$. Also note that the optimal trajectories for all involved players are straight lines and Ω is convex, implying that whether $\tilde{P}_{\hat{m}_1}$ lies in or out of Ω does not make a difference for $P_{\hat{m}_1}$ to protect the target region Ω_{tar} as it can move to any point in Ω along the straight line in Ω. Actually, the concept of virtual pursuer is introduced only for a better understanding of the barrier construction when the pursuer lies in the target region, because we find this mirror property first and then define the virtual pursuer. For a good presentation, we just introduce the virtual pursuer first in this article. Similarly, the case of multiple pursuers can also be verified. Thus, we finish the proof. □

The main result in this section is now given, which provides an efficient way to construct the barrier under Assumptions 1 and 3 by projecting this problem into the field of the former section.

Corollary 1 (Barrier for Relaxed Initial Deployment): Consider the system (1) and suppose that Assumptions 1, 3, and 4 hold. For a pursuit coalition k, let $\mathcal{X}_{k,1}^0$ and $\mathcal{X}_{k,2}^0$ (maybe empty) denote the initial sets of its pursuers who lie in Ω_{play} and Ω_{tar} respectively. By one-to-one mapping of $\mathcal{X}_{k,2}^0$, a set of virtual pursuers can be obtained and denote it by $\tilde{\mathcal{X}}_{k,2}^0$. Then, $\mathcal{B}^{n_k}(\mathcal{X}_k^0) = \mathcal{B}^{n_k}(\mathcal{X}_{k,1}^0 \cup \tilde{\mathcal{X}}_{k,2}^0)$ holds, where $\mathcal{B}^{n_k}(\mathcal{X}_{k,1}^0 \cup \tilde{\mathcal{X}}_{k,2}^0)$ can be computed by Theorem 4.

Proof: Since all players in $\mathcal{X}_{k,1}^0 \cup \tilde{\mathcal{X}}_{k,2}^0$ lie in $\Omega_{\text{play}} \cup \mathcal{T}$, this corollary is obtained by Lemma 4 and Theorem 4. □

V. Pursuit Task Assignment

An optimal task assignment scheme for the pursuit team to guarantee the most evaders intercepted by matching pursuit coalitions with evaders, will be investigated. Intuitively, for every evader, we want to designate a pursuit coalition which can make sure of capturing it. In view of the characteristics of winning regions, the selection of an adequate pursuit coalition can be realized by checking if this evader lies in the capturable region of this pursuit coalition, namely, $\mathcal{W}_P^{n_k}$. In this way, rich prior information about which evaders can be captured by a specified pursuit coalition, is collected. Then, pursuit coalitions can

be matched with evaders one-by-one such that the most evaders are captured. Finally, this maximum matching is formulated as a simplified 0-1 integer programming problem instead of solving a constrained bipartite matching problem [54].

Let $G = (P, E, \mathcal{E})$ denote an undirected bipartite graph, consisting of two independent sets P, E of nodes, and a set $\mathcal{E}$ of unordered pairs of nodes called edges each of which connects a node in P to one in E. In this case, we take $P = \{1, 2, \ldots, 2^{N_p} - 1\}$, representing all pursuit coalitions, and $E = \{1, 2, .., N_e\}$ on behalf of all evaders. An edge from node i in P to node j in E is denoted by e_{ij}, referring to using pursuit coalition i to intercept evader E_j. Define $e_{ij} \in \mathcal{E}$ if pursuit coalition i can guarantee the capture of evader E_j in Ω_{play} or $\mathcal{T}$; otherwise, $e_{ij} \notin \mathcal{E}$. Thus, by computing the barrier for every pursuit coalition, all edges contained in $\mathcal{E}$ can be found.

Traditionally, a subset $M \subseteq \mathcal{E}$ is said to be a matching if no two edges in M are incident to the same node, and our goal is to find a matching containing maximum number of edges, namely, maximum number of evader nodes, as one edge must correspond to one evader and one pursuit coalition and the definition of the matching guarantees that no two edges are connected to the same node. However, note that every pursuer can appear in atmost one pursuit coalition when the interception scheme is executed. Thus, the pursuit coalitions containing atleast one same pursuer cannot coexist, which results in a constrained bipartite matching problem. To solve it, this problem is transformed into a 0-1 integer programming.

Before proceeding with this transformation, the following lemma is presented, which will dramatically decrease the complexity of the 0-1 integer programming proposed later.

Lemma 5 (Degeneration of Pursuit Coalition): For any pursuit coalition k with $n_k \geq 3$, if there exists an evader E_j such that $\mathbf{x}^0_{E_j} \in \mathcal{W}^{n_k}_P$, then there must exist a pursuit subcoalition k_1 of k satisfying $n_{k_1} = 2$ and $\mathbf{x}^0_{E_j} \in \mathcal{W}^{n_{k_1}}_P$.

Proof: Note that Theorem 3 manifests a special feature of the barrier that its every part is only associated with at most two pursuers as (36) shows. Even for the part F^3, one can split it into two parts both of which are only associated with two pursuers. Thus, if a pursuit coalition k can guarantee to capture an evader, then there must exist an its two-pursuer subcoalition which can also guarantee the capture of this evader. □

Remark 4: From Lemma 5, it can be stated that any maximum matching can be reduced to a simpler version in which every pursuit coalition contains at most two pursuers. Therefore, seeking for a maximum matching in the class of this simple version suffices to obtain a matching that is global optimal in the sense of the most evaders intercepted.

Remark 5: Although it follows from Lemma 5 and Remark 4 that the pursuit coalitions with more than two pursuers are not necessary in the maximum matching, the analysis for general pursuit coalitions in Section IV-D can provide instructions to determine the capturable and uncapturable regions of multiple pursuers with any numbers when pursuing one evader. Additionally, this result can also help to deploy the pursuers such that their capturable region is desirable, as sometimes the pursuit team should position its members before an evader occurs. More importantly, it is Theorem 3 that reveals the degeneration of the pursuit coalition described in Lemma 5.

Thus, in the following discussion, attention will be focused on this specific class of pursuit coalitions with at most two pursuers, and due to its crucial role in extracting out an optimal task assignment, it is stated formally as follows.

Definition 8 (Execution Pursuit Coalition): A pursuit coalition k is called an execution pursuit coalition, if $n_k = 1$ or $n_k = 2$.

It can be verified that the set of execution pursuit coalitions consists of N_p one-pursuer coalitions and $N_p(N_p - 1)/2$ two-pursuer coalitions. For notational convenience, define $N_v = N_e(N_p + N_p(N_p - 1)/2) = N_e N_p(N_p + 1)/2$.
According to the barrier construction in Section IV, the following prior information vector can be acquired.

Definition 9 (Prior Information Vector): For P_i, define $\boldsymbol{r}^1_i = [r^1_i(1), \ldots, r^1_i(N_e)] \in \mathbb{R}^{N_e}$, where for $j = 1, \ldots, N_e$, set $r^1_i(j) = 0$ if $\mathbf{x}^0_{E_j} \in \mathcal{W}^1_E(\mathbf{x}^0_{P_i})$, that is, P_i cannot guarantee to capture E_j prior to its arrival in $\mathcal{T}$; otherwise, set $r^1_i(j) = 1$. Similarly, for P_{i1} and P_{i2}, define $\boldsymbol{r}^2_{i1,i2} = [r^2_{i1,i2}(1), \ldots, r^2_{i1,i2}(N_e)] \in \mathbb{R}^{N_e}$, where for $j = 1, \ldots, N_e$, set $r^2_{i1,i2}(j) = 0$ if $\mathbf{x}^0_{E_j} \in \mathcal{W}^2_E(\mathbf{x}^0_{P_{i1}} \cup \mathbf{x}^0_{P_{i2}})$; otherwise, set $r^2_{i1,i2}(j) = 1$. Then we call this vector $\boldsymbol{r} = [\boldsymbol{r}^1_1, \ldots, \boldsymbol{r}^1_{N_p}, \boldsymbol{r}^2_{1,2}, ...\boldsymbol{r}^2_{1,N_p}, \boldsymbol{r}^2_{2,3}, \ldots, \boldsymbol{r}^2_{N_p-1,N_p}] \in \mathbb{R}^{N_v}$ as prior information vector.

Remark 6: Note that the prior information vector $\boldsymbol{r}$ contains all information by which for any given evader, one can judge whether an execution pursuit coalition can guarantee to capture it. This vector is the only input for the maximum matching.

Let $\boldsymbol{s}^1_i = [s^1_i(1), \ldots, s^1_i(N_e)] \in \mathbb{R}^{N_e}$ denote the strategy vector of P_i. Its elements are either 1 or 0, where $s^1_i(j) = 1$ indicates the assignment of P_i to intercept E_j, and $s^1_i(j) = 0$ means no assignment. Clearly, $\sum_{j=1}^{N_e} s^1_i(j) \leq 1$ must be satisfied, namely, P_i at a time can pursue at most one evader. Let $\boldsymbol{s}^2_{i1,i2} = [s^2_{i1,i2}(1), \ldots, s^2_{i1,i2}(N_e)] \in \mathbb{R}^{N_e}$ denote the strategy vector of the pursuit pair $\{P_{i1}, P_{i2}\}$. Its elements are either 1 or 0. Specifically, $s^2_{i1,i2}(j) = 1$ indicates that the pursuit pair $\{P_{i1}, P_{i2}\}$ cooperates to intercept E_j, and $s^2_{i1,i2}(j) = 0$ means no assignment. Obviously, $\sum_{j=1}^{N_e} s^2_{i1,i2}(j) \leq 1$.

Denote the joint strategy vector of all one-pursuer pursuit coalitions by $\boldsymbol{s}^1 = [\boldsymbol{s}^1_1, \ldots, \boldsymbol{s}^1_{N_p}] \in \mathbb{R}^{N_p N_e}$, and denote $\boldsymbol{s}^2 = [\boldsymbol{s}^2_{1,2}, \ldots, \boldsymbol{s}^2_{1,N_p}, \boldsymbol{s}^2_{2,3}, \ldots, \boldsymbol{s}^2_{N_p-1,N_p}] \in \mathbb{R}^{N_e N_p(N_p-1)/2}$ as the joint strategy vector of all two-pursuer pursuit coalitions. Thus $\boldsymbol{z} = [\boldsymbol{s}^1, \boldsymbol{s}^2]^{\mathsf{T}} \in \mathbb{R}^{N_v \times 1}$ denotes all execution pursuit coalitions' strategy vector.

Let $\text{ones}(m, n)$ denote the $m \times n$ matrix each element of which is 1, $\text{zeros}(m, n)$ denote the $m \times n$ zero matrix, I_n denote the identity matrix of size n, $\otimes$ denote the Kronecker product, and $\mathcal{X}^0_P, \mathcal{X}^0_E$ denote the initial positions of all pursuers and all evaders, respectively.

Now, the main result of this section is presented as follows, which gives a maximum matching solution by solving a 0-1 integer programming.

Theorem 5 (Maximum Matching): Consider the system (1) and suppose that Assumptions 1, 3, and 4 hold. Given $\mathcal{X}^0_P$ and $\mathcal{X}^0_E$, the number q of the evaders which the pursuit team can

Algorithm 2: (Matrix for Inequality Constraint).

Input: N_p, N_e, and $A_3 \leftarrow$null matrix.
if $N_p \geq 2$ **then**
for $i \in \{1, 2, \ldots, N_p\}$ **do**
  temp $\leftarrow$null matix
  for $j \in \{1, 2, \ldots, N_p(N_p-1)/2\}$ **do**
    tag $\leftarrow 0$
    for $k \in \{1, 2, \ldots, i-1\} (i \geq 2)$ **do**
      if $j == i - k + (k-1)(N_p - k/2)$ **then**
        tag $\leftarrow 1$, **break**
      end if
    end for
    if $j \geq (i-1)(N_p - i/2) + 1$ &&
      $j \leq i(N_p - (i+1)/2)$ **then**
      tag $\leftarrow 1$
    end if
    temp $\leftarrow$ [temp, tag]
  end for
  $A_3 \leftarrow [A_3; \text{temp}]$
end for
$A_3 \leftarrow A_3 \otimes \text{ones}(1, N_e)$
end if
$A_3 \leftarrow [I_{N_p} \otimes \text{ones}(1, N_e), A_3]$
Output: A_3.

guarantee to prevent from reaching the target region Ω_{tar} is given by

$$\begin{aligned} q &= \text{maximize } \boldsymbol{c}^{\mathsf{T}}\boldsymbol{z} \\ &\quad \text{s. t. } A_1\boldsymbol{z} \leq \boldsymbol{b}_1, A_2\boldsymbol{z} \leq \boldsymbol{b}_2, A_3\boldsymbol{z} \leq \boldsymbol{b}_3 \\ \boldsymbol{z} &= [\boldsymbol{s}^1, \boldsymbol{s}^2]^{\mathsf{T}} = [z(1), \ldots, z(N_v)]^{\mathsf{T}}, \quad z(i) = 0, 1 \end{aligned} \tag{50}$$

and the maximum matching is given by $\boldsymbol{z}^* = \text{argmax}_{\boldsymbol{z}}(\boldsymbol{c}^{\mathsf{T}}\boldsymbol{z})$. The parameter matrixes and vectors are defined as follows:

$$\boldsymbol{c} = \text{ones } (N_v, 1), \boldsymbol{b}_1 = \boldsymbol{r}^{\mathsf{T}}, A_1 = I_{N_v}, \boldsymbol{b}_2 = \text{ones } (N_e, 1)$$
$$A_2 = \text{ones } (1, N_v/N_e) \otimes I_{N_e}, \boldsymbol{b}_3 = \text{ones}(N_p, 1)$$

and A_3 is computed by Algorithm 2 presented as follows.

Proof: Note that the objective function is the number of evaders which are assigned execution pursuit coalitions, that is, the number of the evaders to be captured. The first inequality constraint in (50) represents that the prior information must be satisfied. In other words, assign an adequate execution pursuit coalition to capture an evader. The second inequality constraint indicates that each evader is assigned at most one pursuit coalition, and the third one restricts that each pursuer can occur at most one pursuit coalition when the game runs. It can be verified that Algorithm 2 can find all execution pursuit coalitions which contain a specific pursuer. Thus, this 0-1 integer programming is solvable. □

Remark 7: It can be observed that q is unique, while the maximum matching $\boldsymbol{z}^*$ may have multiple solutions. Moreover, the original matching is a $(2^{N_p} - 1) \times N_e$ constrained bipartite matching problem, which is a NP-problem. However, the maximum matching given by Theorem 5 is simplified a lot with N_v variables and $N_v + N_e + N_p$ inequality constraints. The first inequality constraint in (50) will be simplified a lot when $\boldsymbol{r}$ contains many zero elements.

Definition 10 (Maximum Matching Pairs): For a maximum matching $\boldsymbol{z}^* = [\boldsymbol{s}^{1*}, \boldsymbol{s}^{2*}]^{\mathsf{T}}$, define the sets of matching pairs:

$$M^1(\boldsymbol{z}^*) = \left\{(i,j) \middle| s_i^{1*}(j) = 1, 1 \leq i \leq N_p, 1 \leq j \leq N_e\right\}$$

$$M^2(\boldsymbol{z}^*) = \left\{(i1, i2, j) \middle| s_{i1,i2}^{2*}(j) = 1, 1 \leq i1 < i2 \leq N_p \right.$$
$$\left. 1 \leq j \leq N_e\right\}.$$

Note that $M^1(\boldsymbol{z}^*)$ represents all one-to-one matching pairs in $\boldsymbol{z}^*$, and $M^2(\boldsymbol{z}^*)$ represents all two-to-one matching pairs.

VI. Simulation Results

In this section, simulation results are presented to illustrate the previous theoretical developments. Assume that $v_P = 1$ m/s, $v_E = 0.7$ m/s, namely, $\alpha = 0.7$. Computations are done in Matlab R2016b on a laptop with a Core i7-8550U processor with 16 GB of memory.

Case 1: $N_p = 5$ and $N_e = 6$. Fig. 9 shows the barrier and winning regions for all pursuit coalitions, namely, their capturable and uncapturable regions, where Fig. 9(a) and (e) refer to all one-pursuer pursuit coalitions and five-pursuer pursuit coalition, respectively. For clarity, only two barriers and winning regions are depicted for two-pursuer, three-pursuer, and four-pursuer pursuit coalitions in Fig. 9(b)–(d), respectively. The computation of 31 barriers takes approximately 0.984 s, where every barrier consists of 300 points. Note that since each barrier we construct is analytical, most of the time consumption is due to the computation of 300 points on each barrier, the determination of active pursuers in each coalition and the intersection process between $\breve{\mathcal{B}}^{n_k}$ and Ω_{play}.

Fig. 9(e) also shows the maximum matching from the known barrier and winning regions, including two one-to-one matching pairs and one two-to-one matching pair. Thus, the maximum matching is of size 3. This guarantees that if each pursuer occurring in the maximum matching plays optimally against the evader matched by the maximum matching, this matched evader will be captured before reaching $\mathcal{T}$. The computation of solving a 0-1 integer programming for the maximum matching takes approximately 0.025 s. Moreover, one-pursuer coalitions in Fig. 9(a) indicate that the maximum matching with only one-to-one matching pairs is of size 2. Thus, the size of the maximum matching for this problem cannot exceed 3, because if this size is 4 or 5, the number of one-to-one matching pairs must be more than 2. In Fig. 9(e), we obtain a matching of size 3. Therefore, this analysis specialized for this problem further validates that the matching computed by our method is optimal in the sense of the most evaders captured.

If the methods in [9], [28], and [29] are applied to this task assignment under the same assumption and situation, one can only obtain the results in Fig. 9(a), as these methods only

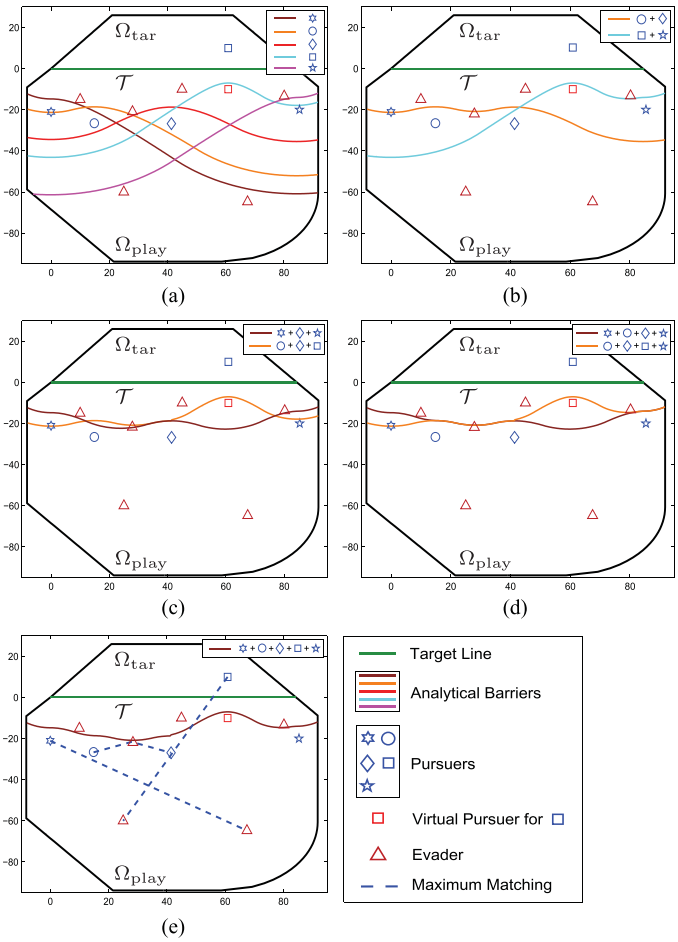

Fig. 9. Five pursuers versus six evaders. (a)–(e) Computation of the barrier and winning regions for all pursuit coalitions when facing one evader: (a) all one-pursuer pursuit coalitions; (b) two-pursuer pursuit coalitions (only two are depicted); (c) three-pursuer pursuit coalitions (only two are depicted); (d) four-pursuer pursuit coalitions (only two are depicted); (e) five-pursuer pursuit coalition, also showing the generated maximum matching: two one-to-one matching pairs and one two-to-one matching pair. Thus, the pursuit team currently can guarantee to capture at most three evaders in Ω_{play}.

construct the barrier for one pursuer versus one evader cases. Thus, it can be observed from Fig. 9(a) that the maximum matching is of size 2, that is, the two evaders with minimum y-coordinates can be matched by two pursuers while no pursuer can capture any one of the other four evaders individually. As for the work [38], it can only construct the barrier for two pursuers in the square domain, and the pursuer in rectangular mark in the target region is also beyond the scope of [38]. Thus, it cannot construct the barrier for this situation.

Case 2: $N_p = 3$ and $N_e = 2$. This example is introduced for showing that the maximum matching based on analytical barriers proposed in this article is not a trivial matching and different from assigning two closest pursuers to each evader, as Fig. 10 illustrates. In Fig. 10(a), the barriers for only-P_1, only-P_2 and P_1–P_2 pair are drawn in brown, orange, and red curves respectively, where part of the red curve coincides with parts of the other two curves. It can be observed that the blue region is the set of initial positions from which a single evader

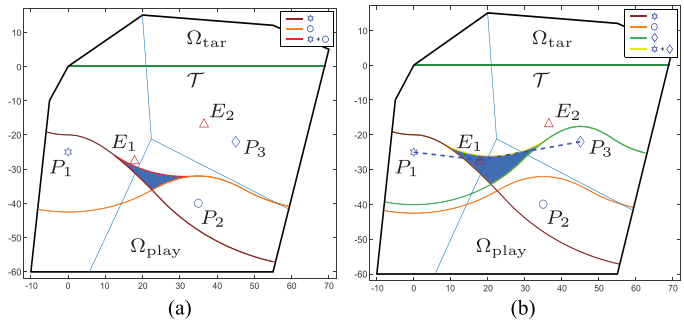

Fig. 10. Three pursuers versus two evaders. (a)The barriers for only-P_1, only-P_2 and P_1–P_2 pair, where the blue region is the set of initial positions from which a single evader can be captured before reaching Ω_{tar} only by P_1–P_2 pair with cooperation, while any one of P_1 and P_2 fails to do by itself. (b) The barriers for only-P_1, only-P_2, only-P_3, and P_1–P_3 pair, where the blue region is the set of initial positions from which a single evader can be captured before reaching Ω_{tar} only by P_1–P_3 pair with cooperation, while any one of P_1 and P_3 fails to do by itself. P_3 dominates P_2 in barrier construction. It also shows the generated maximum matching: one two-to-one matching pair. The blue straight lines are the Voronoi partition lines associated with three pursuers.

can be captured before reaching Ω_{tar} only by P_1–P_2 pair with cooperation, while any one of two pursuers fails to do by itself. In Fig. 10(b), the similar results for P_1 and P_3 are presented. As for P_2 and P_3, P_3 dominates P_2 in barrier construction, because the barrier related P_2 is totally contained in P_3's pursuer winning region. Thus, the barrier for the triple P_1–P_2–P_3 is the same as the barrier for the pair P_1–P_3. The blue straight lines are the Voronoi partition lines associated with three pursuers.

From the above analysis and Fig. 10, E_2 can guarantee to reach Ω_{tar} and E_1 can only be captured by P_1–P_3 pair. Thus, the maximum matching is of size 1 and shown in Fig. 10(b). Although P_1 and P_2 are both closer to E_1 than P_3, our maximum matching reveals that P_3 must be employed to capture E_1. Additionally, although E_2 is closer to P_3 than E_1, P_3 is still assigned to intercept a farther evader, which is not an intuitive assignment. The computation for these barriers takes approximately 0.023 s where every barrier consists of 300 points, and the computation for the maximum matching takes approximately 0.012 s.

VII. Conclusion

A. Conclusions

This article considered a multiplayer RA game in a general convex domain. The key achievement was providing an analytical description of the winning regions when each possible pursuit coalition competed with one evader. Furthermore, an interception scheme involving pursuer-evader matching was generated for the pursuit team such that the most evaders could be captured before entering the target region. The constructed barrier, splitting the winning regions, showed that atmost two pursuers are needed to intercept one evader if the capture was possible, greatly simplifying the matching search.

The winning regions from the whole pursuit team and one evader case also could help the evasion team to determine which evaders could enter the target region or escape from the play region definitely, no matter what strategy the pursuit team used.

Then these evaders would get more attention from the evasion team and be chosen as key mission performers. More generally, this result could provide guarantees on goal satisfaction and safety of optimal system trajectories for safety-critical systems, where a group of vehicles aimed to reach their destinations in the presence of dynamic obstacles.

The results in this article were almost analytical and applicable for real-time updates. More importantly, all possible pursuit coalitions were considered and our results were optimal in the sense from most of the evaders intercepted.

B. Future Work

All players considered in this article moved with simple motion and were able to turn instantaneously. In future work, more practical and complex dynamic models will be considered, for example, those of the Isaacs–Dubins car. Extending the results obtained in general convex domains to nonconvex domains is another worth-pursuing direction, and extracting out some conservative results is straightforward, such as, approximating the nonconvex domain with an appropriate convex domain. In view of the limited communication and computing power of a single player, another interesting and promising possibility for future extension is to consider distributed multiplayer RA games, which is the focus of our following research.

REFERENCES

[1] T. Basar and G. J. Olsder, *Dynamic Noncooperative Game Theory*. New York, NY, USA: SIAM, 1999.

[2] T. H. Chung, G. A. Hollinger, and V. Isler, "Search and pursuit-evasion in mobile robotics," *Auton. Robots*, vol. 31, no. 4, pp. 299–316, Jul. 2011.

[3] V. Shaferman and T. Y. Shima, "A cooperative differential game for imposing a relative intercept angle," in *Proc. AIAA Guid., Navigat., Control Conf.*, 2017, pp. 1015–1039.

[4] X. Dong and G. Hu, "Time-varying formation tracking for linear multiagent systems with multiple leaders," *IEEE Trans. Autom. Control*, vol. 62, no. 7, pp. 3658–3664, Jul. 2017.

[5] J. Ding, M. Kamgarpour, S. Summers, A. Abate, J. Lygeros, and C. Tomlin, "A stochastic games framework for verification and control of discrete time stochastic hybrid systems," *Automatica*, vol. 49, no. 9, pp. 2665–2674, 2013.

[6] Z. Zhou, R. Takei, H. Huang, and C. J. Tomlin, "A general, open-loop formulation for reach-avoid games," in *Proc. IEEE 51st Conf. Decis. Control*, 2012, pp. 6501–6506.

[7] D. Panagou and V. Kumar, "Cooperative visibility maintenance for leader–follower formations in obstacle environments," *IEEE Trans. Robot.*, vol. 30, no. 4, pp. 831–844, Aug. 2014.

[8] S. Pan, H. Huang, J. Ding, and W. Zhang, "Pursuit, evasion and defense in the plane," in *Proc. Amer. Control Conf.*, 2012, pp. 4167–4173.

[9] M. Chen, Z. Zhou, and C. J. Tomlin, "Multiplayer reach-avoid games via pairwise outcomes," *IEEE Trans. Autom. Control*, vol. 62, no. 3, pp. 1451–1457, Mar. 2017.

[10] S. Y. Hayoun and T. Shima, "On guaranteeing point capture in linear n-on-1 endgame interception engagements with bounded controls," *Automatica*, vol. 85, no. Supplement C, pp. 122–128, 2017.

[11] H. Raslan, H. Schwartz, and S. Givigi, "A learning invader for the "guarding a territory" game," *J. Intell. Robot. Syst.*, vol. 83, no. 1, pp. 55–70, Jan. 2016.

[12] H. Huang, J. Ding, W. Zhang, and C. J. Tomlin, "Automation-assisted capture-the-flag: A differential game approach," *IEEE Trans. Control Syst. Technol.*, vol. 23, no. 3, pp. 1014–1028, May 2015.

[13] W. Scott and N. E. Leonard, "Pursuit, herding and evasion: A three-agent model of caribou predation," in *Proc. Amer. Control Conf.*, Jun. 2013, pp. 2978–2983.

[14] E. Garcia, D. W. Casbeer, and M. Pachter, "Design and analysis of state-feedback optimal strategies for the differential game of active defense," *IEEE Trans. Autom. Control*, vol. 64, no. 2, pp. 1014–1028, Feb. 2019.

[15] S. Chung, A. A. Paranjape, P. Dames, S. Shen, and V. Kumar, "A survey on aerial swarm robotics," *IEEE Trans. Robot.*, vol. 34, no. 4, pp. 837–855, Aug. 2018.

[16] B. P. Gerkey and M. J. Matari, "A formal analysis and taxonomy of task allocation in multi-robot systems," *Int. J. Robot. Res.*, vol. 23, no. 9, pp. 939–954, 2004.

[17] S. Chopra, G. Notarstefano, M. Rice, and M. Egerstedt, "A distributed version of the hungarian method for multirobot assignment," *IEEE Trans. Robot.*, vol. 33, no. 4, pp. 932–947, Aug. 2017.

[18] H. Choi, L. Brunet, and J. P. How, "Consensus-based decentralized auctions for robust task allocation," *IEEE Trans. Robot.*, vol. 25, no. 4, pp. 912–926, Aug. 2009.

[19] K. Zhou and S. I. Roumeliotis, "Multirobot active target tracking with combinations of relative observations," *IEEE Trans. Robot.*, vol. 27, no. 4, pp. 678–695, Aug. 2011.

[20] B. Xue, A. Easwaran, N. J. Cho, and M. Franzle, "Reach-avoid verification for nonlinear systems based on boundary analysis," *IEEE Trans. Autom. Control*, vol. 62, no. 7, pp. 3518–3523, Jul. 2017.

[21] M. Chen, S. L. Herbert, M. S. Vashishtha, S. Bansal, and C. J. Tomlin, "Decomposition of reachable sets and tubes for a class of nonlinear systems," *IEEE Trans. Autom. Control*, vol. 63, no. 11, pp. 3675–3688, Nov. 2018.

[22] K. G. Vamvoudakis and F. L. Lewis, "Multi-player non-zero-sum games: Online adaptive learning solution of coupled Hamilton-Jacobi equations," *Automatica*, vol. 47, no. 8, pp. 1556–1569, 2011.

[23] Z. Zhou, J. Ding, H. Huang, R. Takei, and C. Tomlin, "Efficient path planning algorithms in reach-avoid problems," *Automatica*, vol. 89, pp. 28–36, 2018.

[24] R. Isaacs, *Differential Games*. New York, NY, USA: Wiley, 1967.

[25] K. Weekly, A. Tinka, L. Anderson, and A. M. Bayen, "Autonomous river navigation using the Hamilton– Jacobi framework for underactuated vehicles," *IEEE Trans. Robot.*, vol. 30, no. 5, pp. 1250–1255, Oct. 2014.

[26] C. J. Tomlin, J. Lygeros, and S. S. Sastry, "A game theoretic approach to controller design for hybrid systems," *Proc. IEEE*, vol. 88, no. 7, pp. 949–970, Jul. 2000.

[27] I. M. Mitchell, A. M. Bayen, and C. J. Tomlin, "A time-dependent Hamilton-Jacobi formulation of reachable sets for continuous dynamic games," *IEEE Trans. Autom. Control*, vol. 50, no. 7, pp. 947–957, Jul. 2005.

[28] K. Margellos and J. Lygeros, "Hamilton-Jacobi formulation for reach-avoid differential games," *IEEE Trans. Autom. Control*, vol. 56, no. 8, pp. 1849–1861, Aug. 2011.

[29] J. F. Fisac, M. Chen, C. J. Tomlin, and S. S. Sastry, "Reach-avoid problems with time-varying dynamics, targets and constraints," in *Proc. 18th Int. Conf. Hybrid Syst.: Comput. Control*, New York, NY, USA, 2015, pp. 11–20.

[30] J. Lewin, *Differential Games: Theory and Methods for Solving Game Problems with Singular Surfaces*. London, U.K.: Springer-Verlag, 2012.

[31] S. D. Bopardikar, F. Bullo, and J. P. Hespanha, "A cooperative homicidal chauffeur game," *Automatica*, vol. 45, no. 7, pp. 1771–1777, 2009.

[32] R. Yan, Z. Shi, and Y. Zhong, "Escape-avoid games with multiple defenders along a fixed circular orbit," in *Proc. 13th IEEE Int. Conf. Control Autom.*, 2017, pp. 958–963.

[33] R. Lopez-Padilla, R. Murrieta-Cid, I. Becerra, G. Laguna, and S. M. LaValle, "Optimal navigation for a differential drive disc robot: A game against the polygonal environment," *J. Intell. Robot. Syst.*, vol. 89, no. 1, pp. 211–250, Jan. 2018.

[34] A. Pierson, Z. Wang, and M. Schwager, "Intercepting rogue robots: An algorithm for capturing multiple evaders with multiple pursuers," *IEEE Robot. Autom. Lett.*, vol. 2, no. 2, pp. 530–537, Apr. 2017.

[35] Z. Zhou, W. Zhang, J. Ding, H. Huang, D. M. Stipanovic, and C. J. Tomlin, "Cooperative pursuit with Voronoi partitions," *Automatica*, vol. 72, pp. 64–72, Oct. 2016.

[36] E. Bakolas and P. Tsiotras, "Relay pursuit of a maneuvering target using dynamic Voronoi diagrams," *Automatica*, vol. 48, no. 9, pp. 2213–2220, Sep. 2012.

[37] M. V. Ramana and M. Kothari, "Pursuit strategy to capture high-speed evaders using multiple pursuers," *J. Guid. Control Dyn.*, vol. 40, pp. 139–149, 2017.

[38] R. Yan, Z. Shi, and Y. Zhong, "Reach-avoid games with two defenders and one attacker: An analytical approach," *IEEE Trans. Cybern.*, vol. 49, no. 3, pp. 1035–1046, Mar. 2019.

[39] D. W. Oyler, P. T. Kabamba, and A. R. Girard, "Pursuit-evasion games in the presence of obstacles," *Automatica*, vol. 65, pp. 1–11, Mar. 2016.

[40] R. Zou and S. Bhattacharya, "On optimal pursuit trajectories for visibility-based target-tracking game," *IEEE Trans. Robot.*, vol. 35, no. 2, pp. 449–465, Apr. 2019.

[41] J. Yu and S. M. LaValle, "Shadow information spaces: Combinatorial filters for tracking targets," *IEEE Trans. Robot.*, vol. 28, no. 2, pp. 440–456, Apr. 2012.
[42] M. Katsev, A. Yershova, B. Tovar, R. Ghrist, and S. M. LaValle, "Mapping and pursuit-evasion strategies for a simple wall-following robot," *IEEE Trans. Robot.*, vol. 27, no. 1, pp. 113–128, Feb. 2011.
[43] N. Noori and V. Isler, "Lion and man with visibility in monotone polygons," *Int. J. Robot. Res.*, vol. 33, no. 1, pp. 155–181, 2014.
[44] D. Bhadauria, K. Klein, V. Isler, and S. Suri, "Capturing an evader in polygonal environments with obstacles: The full visibility case," *Int. J. Robot. Res.*, vol. 31, no. 10, pp. 1176–1189, 2012.
[45] U. Ruiz and R. Murrieta-Cid, "A differential pursuit/evasion game of capture between an omnidirectional agent and a differential drive robot, and their winning roles," *Int. J. Control*, vol. 89, no. 11, pp. 2169–2184, Feb. 2016.
[46] W. Sun and P. Tsiotras, "Pursuit evasion game of two players under an external flow field," in *Proc. Amer. Control Conf.*, 2015, pp. 5617–5622.
[47] R. Zou and S. Bhattacharya, "Visibility-based finite-horizon target tracking game," *IEEE Robot. Autom. Lett.*, vol. 1, no. 1, pp. 399–406, Jan. 2016.
[48] R. Yan, Z. Shi, and Y. Zhong, "Defense game in a circular region," in *Proc. 56th IEEE Conf. Decis. Control*, 2017, pp. 5590–5595.
[49] U. Ruiz, R. Murrieta-Cid, and J. L. Marroquin, "Time-optimal motion strategies for capturing an omnidirectional evader using a differential drive robot," *IEEE Trans. Robot.*, vol. 29, no. 5, pp. 1180–1196, Oct. 2013.
[50] V. Macias, I. Becerra, R. Murrieta-Cid, H. M. Becerra, and S. Hutchinson, "Image feedback based optimal control and the value of information in a differential game," *Automatica*, vol. 90, pp. 271–285, 2018.
[51] S. Bhattacharya and S. Hutchinson, "A cell decomposition approach to visibility-based pursuit evasion among obstacles," *Int. J. Robot. Res.*, vol. 30, no. 14, pp. 1709–1727, 2011.
[52] E. N. Barron, "Reach-avoid differential games with targets and obstacles depending on controls," *Dyn. Games Appl.*, vol. 8, no. 4, pp. 696–712, Dec. 2018.
[53] R. J. Elliott and N. J. Kalton, "The existence of value in differential games," *Memoirs Amer. Math. Soc.*, vol. 126, no. 126, pp. 504–523, 1972.
[54] E. L. Lawler, *Combinatorial Optimization: Networks and Matroids*. North Chelmsford, MA, USA: Courier Corporation, 1976.

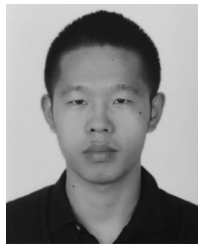

Rui Yan (S'17) received the B.E. degree in automatic control from Beihang University, Beijing, China in 2015. He is currently working toward the Ph.D. degree in robotics and game theory with the Department of Automation at Tsinghua University, Beijing, China.

His research interests focus on multi-agent systems, game theory, multi-agent reinforcement learning, differential games, and robot competition.

Zongying Shi (M'12) received the B.E. degree in control theory and application, the M.E. and Ph.D. degrees in control engineering from Tsinghua University, Beijing, China in 1992, 1994, and 2005, respectively.

Since 1994, she has been with the Department of Automation, Tsinghua University, where she is currently an Associate Professor. Her research interests include multiagent coordination control, simultaneous localization and mapping, and robust control for robots.

Yisheng Zhong received the B.E. degree in control engineering from the Harbin Institute of Technology, Harbin, China, in 1982, the M.E. degree in electronic engineering from the University of Electro-Communications, Tokyo, Japan, in 1985, and the Ph.D. degree in electrical engineering from Hokkaido University, Sapporo, Japan, in 1988.

He was a Postdoctorate Scholar with Tsinghua University, Beijing, China, from 1989 to 1990, and since 1991, he has been with the Department of Automation, Tsinghua University, where he is currently a Professor and also with the Tsinghua National Laboratory for Information Science and Technology. His research interests include robust control, nonlinear control, and differential games.